

A NUCLEAR MAGNETIC RESONANCE  
LINESHAPE STUDY OF  
AN ABC SPIN SYSTEM UNDERGOING  
INTRAMOLECULAR EXCHANGE

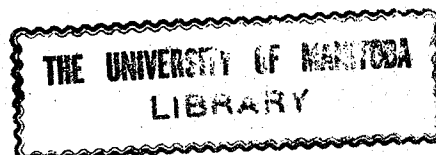
A Thesis  
Submitted to  
The Faculty of Graduate Studies and Research  
at the University of Manitoba  
in Partial Fulfillment  
of the Requirements for the Degree of  
MASTER OF SCIENCE

by

Helen G. Gyulai

Winnipeg, Manitoba

June, 1970



TO MY MOTHER AND FATHER

ACKNOWLEDGEMENTS

My sincere thanks go to Dr. T. Schaefer without whose help and encouragement this thesis could not have been written.

I am grateful to my colleague, Bryan Fuhr, for obtaining the experimental spectra required to carry out this work. I am also grateful to my colleagues, Bruce Goodwin, Christine Shepperd and Rod Wasylshen for many helpful discussions during the course of this work.

I am indebted to the Chemistry Department of the University of Manitoba for financial assistance.

ABSTRACT

The temperature dependence of the rate constant for the hindered internal rotation of the dichloromethyl group in  $\alpha,\alpha,2,4,6$ -pentachlorotoluene in  $\text{CS}_2$  solution was investigated using the steady-state nuclear magnetic resonance technique. The rate constants at nine different temperatures in a  $100^\circ\text{C}$  range were obtained by matching theoretical and experimental spectra. Theoretical spectra were calculated for a large number of rate constants using the computer program DNMR, and the best overall lineshape fits with the experimental spectra were obtained visually. The complete lineshape theory devised by Binsch, on which the program DNMR is based, is described and the calculations are done in detail for an exchanging two-spin system. Activation parameters for the rate process were calculated by using the Arrhenius and Eyring rate equations. The activation parameters for the  $\text{CS}_2$  solution are as follows:

$E_a = 14.22 \pm 0.27$  kilocalories mole $^{-1}$ ,  $\Delta H^\ddagger = 13.69 \pm 0.27$  kilocalories mole $^{-1}$ , and  $\Delta S^\ddagger = -4.38 \pm 1.0$  e.u. The hindered rotation in  $\alpha,\alpha,2,4,6$ -pentachlorotoluene in toluene- $d_8$  and methylcyclohexane solutions was studied by Fuhr. The rate data obtained for the three solutions were combined giving the following results for the activation parameters:

$E_a = 14.24 \pm 0.27$  kilocalories mole $^{-1}$ ,  $\Delta H^\ddagger = 13.68 \pm 0.27$  kilocalories mole $^{-1}$ , and  $\Delta S^\ddagger = -4.37 \pm 1.0$  e.u.

TABLE OF CONTENTS

CHAPTER		PAGE
	Acknowledgements.....	iii
	Abstract.....	iv
	Table of Contents.....	v
	List of Tables.....	vii
	List of Figures.....	viii
I	INTRODUCTION.....	1
II	THE UNIFIED LINESHAPE THEORY.....	3
	A. Introduction.....	3
	B. The Liouville Representation of Quantum Mechanics.....	4
	C. Derivation of the Lineshape Equation.....	13
	i) The State Vector.....	13
	ii) The Equation of Motion..	15
	iii) The Liouville Operator..	18
	iv) The Steady-State Condi- tion.....	21
	D. Computational Procedure and the Description of the Com- puter Program.....	31
III	APPLICATION OF THE THEORY TO AN ABC SPIN SYSTEM.....	40
	A. Introduction.....	40
	B. Experimental Procedure and Analysis of Spectra.....	43
	C. Calculation of the Rate Con- stants.....	49
	D. Calculation of the Thermody- namic Parameters.....	61

CHAPTER		PAGE
IV	DISCUSSION.....	69
	A. The Energy Barrier to Rotation.....	69
	B. Errors.....	75
V	CONCLUSION.....	82
VI	SUGGESTIONS FOR FUTURE RESEARCH.....	83
	BIBLIOGRAPHY.....	86
	APPENDIX I: .....	88
	APPENDIX II: .....	91

LIST OF TABLES

TABLE		PAGE
1	Chemical shifts and coupling constants of some low temperature spectra as analysed by LAOCN3.....	46
2	The static parameters used in calculating the lineshapes.....	48
3	The rate constants and estimated errors for the hindered rotation in $\alpha,\alpha,2,4,6$ -pentachlorotoluene at a series of temperatures.....	60
4	The data required for calculating the thermodynamic parameters.....	63
5	Thermodynamic parameters for the hindered rotation in $\alpha,\alpha,2,4,6$ -pentachlorotoluene in three solutions.....	68
6	Maximum and minimum values for the thermodynamic parameters.....	81

LIST OF FIGURES

FIGURE		PAGE
1	The proton magnetic resonance spectrum of $\alpha,\alpha,2,4,6$ -pentachlorotoluene at $-34^{\circ}\text{C}$ , $30^{\circ}\text{C}$ , and $73^{\circ}\text{C}$ .....	44
2	Experimental spectrum at $-34^{\circ}\text{C}$ and the corresponding calculated spectrum..	50
3	Experimental spectrum at $-15^{\circ}\text{C}$ and the corresponding calculated spectrum..	51
4	Experimental spectrum at $0^{\circ}\text{C}$ and the corresponding calculated spectrum.....	52
5	Experimental spectrum at $10^{\circ}\text{C}$ and the corresponding calculated spectrum.....	53
6	Experimental spectrum at $18^{\circ}\text{C}$ and the corresponding calculated spectrum.....	54
7	Experimental spectrum at $30^{\circ}\text{C}$ and the corresponding calculated spectrum.....	55
8	Experimental spectrum at $47^{\circ}\text{C}$ and the corresponding calculated spectrum.....	56
9	Experimental spectrum at $62^{\circ}\text{C}$ and the corresponding calculated spectrum.....	57
10	Experimental spectrum at $73^{\circ}\text{C}$ and the corresponding calculated spectrum.....	58
11	Arrhenius plot for the hindered rotation in $\alpha,\alpha,2,4,6$ -pentachlorotoluene in 15 mole % $\text{CS}_2$ solution.....	64
12	Eyring plot for the hindered rotation in $\alpha,\alpha,2,4,6$ -pentachlorotoluene in 15 mole % $\text{CS}_2$ solution.....	65
13	Arrhenius plot for the hindered rotation of $\alpha,\alpha,2,4,6$ -pentachlorotoluene in the three solvents $\text{CS}_2$ , toluene- $\text{d}_8$ , and methylcyclohexane.....	66
14	Eyring plot for the hindered rotation in $\alpha,\alpha,2,4,6$ -pentachlorotoluene in the three solvents $\text{CS}_2$ , toluene- $\text{d}_8$ , and methylcyclohexane.....	67



FIGURE	PAGE
15 The potential energy of $\alpha,\alpha,2,6$ -tetrachlorotoluene as a function of degree of rotation of the dichloromethyl group, as calculated from a modified Buckingham potential energy function.....	72
16 The room temperature proton magnetic resonance spectrum of $\alpha,\alpha$ -dibromo-2,6-dichlorotoluene at 60 MHz.....	84

CHAPTER I

INTRODUCTION

The use of nuclear magnetic resonance (NMR) techniques in the study of reaction rates and the deduction of thermodynamic parameters for chemical reactions at equilibrium has become widespread in recent years (1,2). The NMR spectrum of a system undergoing chemical exchange is dependent on the rate of exchange, if this rate lies within the frequency range of an NMR experiment ( $10^{-1}$  to  $10^4$  sec $^{-1}$ ). The procedure used in steady state NMR experiments is to match experimental spectra obtained over a range of temperatures to theoretical spectra in which the variable parameter is the rate constant for the exchange. The data thus obtained may be used to calculate the various activation parameters by employing either the Arrhenius or the Eyring rate equations.

The main difficulty encountered in the procedure involves the derivation of a suitable equation for the lineshape. The first detailed treatment of exchange phenomena, based on modifying the Bloch equations, was presented by Gutowsky, McCall, and Slichter (3) and elaborated in later papers by Gutowsky and co-workers (4,5). Since spin-spin coupling has no classical analogue, these earlier theories were de facto inadequate to describe systems complicated by strong spin-spin interactions. A quantum mechanical line shape theory based on the density matrix formalism (6) was devised by Kaplan (7,8) and

Alexander (9,10). Although this theory greatly extends the range of application of NMR to rate studies it is still limited by the fact that it can be applied only to systems undergoing mutual exchange. Johnson modified the theory to include nonmutual exchange phenomena (11,12). Binsch recast the whole density matrix formalism from the Hilbert space representation into the Liouville representation of quantum mechanics (13), which enabled him to describe the lineshape of any system hitherto mentioned by one unified equation (14).

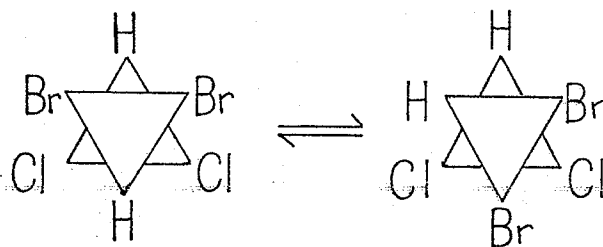
It is the purpose of this thesis to describe in some detail the theory devised by Binsch and to illustrate its application to a tightly coupled three-spin system in which two of the nuclei are undergoing intramolecular mutual exchange. Some of the difficulties and errors encountered in the method will also be discussed.

CHAPTER II

THE UNIFIED LINE SHAPE THEORY

### A. Introduction

The principal aim of this chapter is to present to the reader in a fairly comprehensible manner the theory of NMR line shapes developed in the Liouville representation of quantum mechanics. The emphasis will be placed on clarity and simplicity of presentation rather than on a rigorous mathematical derivation of the theory. The calculation will be done in detail for a two-spin system undergoing intramolecular exchange between two different configurations, as would occur, for example, in the hindered rotation of the tetrasubstituted ethane,  $\text{CHCl}_2\text{CHBr}_2$ :



To give the reader some familiarity with the Liouville representation, the first section of this chapter is devoted to a brief summary of the treatment of this topic done by Fano (13). The final section deals with the reduction of the lineshape equation, developed in section C, to a form amenable to computation. The computer program, DNMR, based on this theory is also given brief attention.

## B. The Liouville Representation of Quantum Mechanics

In quantum mechanics a pure state<sup>1</sup> is identified by a state vector,  $\Psi$ , which is a linear combination of a set of orthonormalized, time-independent eigenvectors of some complete set of operators in Hilbert space:

$$\Psi = \sum_n C_n U_n \quad 1.1$$

The mean value of an operator  $A$  is given by:

$$\begin{aligned} \langle A \rangle &= \langle \Psi | A | \Psi \rangle = \sum_{m,n} \langle C_m U_m | A | C_n U_n \rangle \\ &= \sum_{m,n} A_{mn} C_m^* C_n, \end{aligned} \quad 1.2$$

where

$$A_{mn} = \langle U_m | A | U_n \rangle \quad 1.3$$

A mixed state, or ensemble, is represented by the incoherent superposition of pure states,  $\Psi^i$ , each having a statistical weight  $p^i$ . The mean value of  $A$  for the ensemble is then given by the grand average of mean values corresponding to each pure state:

$$\langle A \rangle = \sum_i p^i \langle A \rangle_i = \sum_i \sum_{m,n} A_{mn} p^i C_m^{i*} C_n^i \quad 1.4$$

---

1. A pure state is characterized by the existence of an experiment which gives a predictable result with certainty.

The density matrix for the system can be defined by the elements<sup>1</sup>:

$$\rho_{nm} = \sum_i p_i^i C_m^{i*} C_n^i, \quad 1.5$$

so that the mean value of A can be written:

$$\langle A \rangle = \sum_{m,n} A_{mn} \rho_{nm} = \text{Tr} (A\rho), \quad 1.6$$

where Tr indicates the trace, or the sum of the diagonal elements.

In the Liouville representation we consider a set of operators  $U^{(j)}$ , with the property:

$$\text{Tr} \{U^{(j)} U^{(k)\dagger}\} = \delta_{jk}, \quad \begin{array}{l} \delta_{jk}=1, \text{ if } j=k \\ \delta_{jk}=0, \text{ if } j \neq k \end{array} \quad 1.7$$

and identify a system by a state vector whose components are the mean values of these operators:

$$\rho_j = \langle U^{(j)\dagger} \rangle = \text{Tr} (U^{(j)\dagger} \rho) = \sum_{m,n} U_{mn}^{(j)*} \rho_{mn} \quad 1.8$$

where, † represents the adjoint.

Because of the orthonormalization condition, equation 1.7, the elements of the operators  $U^{(j)}$  can be laid out in the form of row vectors and these vectors can be regarded as unit coordinate vectors of a vector space, referred to as the Liouville space. All operators in this space can be

---

1. For a full derivation of the density matrix, see references (6) and (15).



represented by the general formula:

$$A = \sum_j A_j^* U^{(j)} = \sum_j A_j U^{(j)\dagger} \quad 1.9$$

The components  $A_j$  are the projections of the vector  $A$  along each coordinate vector  $U^{(j)}$  and hence are given by<sup>1</sup>:

$$A_j = A \cdot U^{(j)} \quad 1.10$$

If the  $U^{(j)}$  are chosen to be Hermitian, then it follows from equation 1.8 that

$$\rho_j = U^{(j)} \rho = \rho \cdot U^{(j)}, \quad 1.11$$

and the representation of the state vector is just a particular case of equation 1.9:

$$\rho = \sum_j \rho_j^* U^{(j)} = \sum_j \rho_j U^{(j)\dagger}$$

The mean value of an operator in this representation can be expressed as the scalar product:

---

1. The dot represents the operation of taking the scalar product of the two vectors. The scalar product defined for vectors is represented by the corresponding matrix product, namely the product from the right of a row vector by a column vector. The  $\cdot$  symbol always implies that if one of the component vectors does not have the correct matrix representation, then its adjoint is to be taken.

$$\langle A \rangle = \sum_j A_j \rho_j^* = \sum_j A_j^* \rho_j = A \cdot \rho \quad 1.13$$

This equation illustrates the fact that in the Liouville representation the mean value of an operator characterizes the projection of  $\rho$  on a very small subspace of the entire space of state vectors. Since the scalar product is independent of the representation, provided both vectors are given in the same representation, it is not necessary to work with the basis set  $U^{(j)}$ , but any set of vectors which span the vector space of interest can be used. In applications to nuclear magnetic resonance lineshapes, it is found that the most convenient set of basis vectors are the eigenvectors of the Zeeman interaction Hamiltonian.

As an illustrative example, the mean value of the "lowering operator",  $I^- = I_x - iI_y$  will be calculated for a two spin system both in the Hilbert space and Liouville representations.

The density matrix of a two spin system is represented in Hilbert space as:

$$\rho = \begin{bmatrix} \rho_{11} & \rho_{12} & \rho_{13} & \rho_{14} \\ \rho_{21} & \rho_{22} & \rho_{23} & \rho_{24} \\ \rho_{31} & \rho_{32} & \rho_{33} & \rho_{34} \\ \rho_{41} & \rho_{42} & \rho_{43} & \rho_{44} \end{bmatrix} \quad 1.14$$

The mean value of the "lowering operator",  $I^- = I_x - iI_y$ , is given by the trace:

$$\langle I^- \rangle = \text{Tr} (I^- \rho) \quad 1.15$$

$$I^- \rho = \begin{bmatrix} 0 & 1 & 1 & 0 \\ 0 & 0 & 0 & 1 \\ 0 & 0 & 0 & 1 \\ 0 & 0 & 0 & 0 \end{bmatrix} \begin{bmatrix} \rho_{11} & \rho_{12} & \rho_{13} & \rho_{14} \\ \rho_{21} & \rho_{22} & \rho_{23} & \rho_{24} \\ \rho_{31} & \rho_{32} & \rho_{33} & \rho_{34} \\ \rho_{41} & \rho_{42} & \rho_{43} & \rho_{44} \end{bmatrix}$$

$$= \begin{bmatrix} \rho_{21} + \rho_{31} & \rho_{22} + \rho_{32} & \rho_{23} + \rho_{33} & \rho_{24} + \rho_{34} \\ \rho_{41} & \rho_{42} & \rho_{43} & \rho_{44} \\ \rho_{41} & \rho_{42} & \rho_{43} & \rho_{44} \\ 0 & 0 & 0 & 0 \end{bmatrix} \quad 1.16$$

$$\text{Tr}(I^- \rho) = \rho_{21} + \rho_{31} + \rho_{42} + \rho_{43} \quad 1.17$$

To characterize the Liouville space for a two spin system, sixteen basis vectors are required. The sixteen product operators:  $E(1)E(2), E(1)I_x(2), E(1)I_y(2), E(1)I_z(2), I_x(1)E(2), I_x(1)I_x(2), I_x(1)I_y(2), I_x(1)I_z(2), I_y(1)E(2), I_y(1)I_x(2), I_y(1)I_y(2), I_y(1)I_z(2), I_z(1)E(2), I_z(1)I_x(2), I_z(1)I_y(2), I_z(1)I_z(2),$

where E is the identity operator and  $I_x$ ,  $I_y$ , and  $I_z$  are the Pauli spin matrices, if properly normalized, can be considered as the unit coordinate vectors of a sixteen dimensional vector space. When laid out in vector form these sixteen operators are<sup>1</sup>:

$$\begin{aligned}
 U^{(1)} &= E(1)E(2) = \frac{1}{2}(1 \ 0 \ 0 \ 0 \ 0 \ 1 \ 0 \ 0 \ 0 \ 0 \ 1 \ 0 \ 0 \ 0 \ 0 \ 1) \\
 U^{(2)} &= E(1)I_x(2) = \frac{1}{2}(0 \ 1 \ 0 \ 0 \ 1 \ 0 \ 0 \ 0 \ 0 \ 0 \ 0 \ 1 \ 0 \ 0 \ 1 \ 0) \\
 U^{(3)} &= E(1)I_y(2) = \frac{1}{2}(0 \ -i \ 0 \ 0 \ i \ 0 \ 0 \ 0 \ 0 \ 0 \ 0 \ -i \ 0 \ 0 \ i \ 0) \\
 U^{(4)} &= E(1)I_z(2) = \frac{1}{2}(1 \ 0 \ 0 \ 0 \ 0 \ -1 \ 0 \ 0 \ 0 \ 0 \ 1 \ 0 \ 0 \ 0 \ 0 \ -1) \\
 U^{(5)} &= I_x(1)E(2) = \frac{1}{2}(0 \ 0 \ 1 \ 0 \ 0 \ 0 \ 0 \ 1 \ 1 \ 0 \ 0 \ 0 \ 0 \ 1 \ 0 \ 0) \\
 U^{(6)} &= I_x(1)I_x(2) = \frac{1}{2}(0 \ 0 \ 0 \ 1 \ 0 \ 0 \ 1 \ 0 \ 0 \ 1 \ 0 \ 0 \ 1 \ 0 \ 0 \ 0) \\
 U^{(7)} &= I_x(1)I_y(2) = \frac{1}{2}(0 \ 0 \ 0 \ -i \ 0 \ 0 \ i \ 0 \ 0 \ -i \ 0 \ 0 \ i \ 0 \ 0 \ 0) \\
 U^{(8)} &= I_x(1)I_z(2) = \frac{1}{2}(0 \ 0 \ 1 \ 0 \ 0 \ 0 \ 0 \ -1 \ 1 \ 0 \ 0 \ 0 \ 0 \ -1 \ 0 \ 0) \\
 U^{(9)} &= I_y(1)E(2) = \frac{1}{2}(0 \ 0 \ -i \ 0 \ 0 \ 0 \ 0 \ -i \ i \ 0 \ 0 \ 0 \ 0 \ i \ 0 \ 0) \\
 U^{(10)} &= I_y(1)I_x(2) = \frac{1}{2}(0 \ 0 \ 0 \ -i \ 0 \ 0 \ -i \ 0 \ 0 \ i \ 0 \ 0 \ i \ 0 \ 0 \ 0) \\
 U^{(11)} &= I_y(1)I_y(2) = \frac{1}{2}(0 \ 0 \ 0 \ -1 \ 0 \ 0 \ 1 \ 0 \ 0 \ 1 \ 0 \ 0 \ -1 \ 0 \ 0 \ 0) \\
 U^{(12)} &= I_y(1)I_z(2) = \frac{1}{2}(0 \ 0 \ -i \ 0 \ 0 \ 0 \ 0 \ i \ i \ 0 \ 0 \ 0 \ 0 \ -i \ 0 \ 0) \\
 U^{(13)} &= I_z(1)E(2) = \frac{1}{2}(1 \ 0 \ 0 \ 0 \ 0 \ 1 \ 0 \ 0 \ 0 \ 0 \ -1 \ 0 \ 0 \ 0 \ 0 \ -1) \\
 U^{(14)} &= I_z(1)I_x(2) = \frac{1}{2}(0 \ 1 \ 0 \ 0 \ 1 \ 0 \ 0 \ 0 \ 0 \ 0 \ 0 \ -1 \ 0 \ 0 \ -1 \ 0) \\
 U^{(15)} &= I_z(1)I_y(2) = \frac{1}{2}(0 \ -i \ 0 \ 0 \ i \ 0 \ 0 \ 0 \ 0 \ 0 \ 0 \ i \ 0 \ 0 \ -i \ 0) \\
 U^{(16)} &= I_z(1)I_z(2) = \frac{1}{2}(1 \ 0 \ 0 \ 0 \ 0 \ -1 \ 0 \ 0 \ 0 \ 0 \ -1 \ 0 \ 0 \ 0 \ 0 \ 1)
 \end{aligned}$$

1.18

---

1. The form of these operators is derived in Appendix I.

It is apparent upon inspection that these vectors satisfy the orthonormalization condition:

$$U^{(j)} \cdot U^{(k)} = \delta_{jk}, \quad \begin{array}{l} \delta_{jk}=1 \text{ if } j=k, \\ \delta_{jk}=0 \text{ if } j \neq k \end{array} \quad 1.19$$

In this representation, the operator  $I^-$  is given by:

$$I^- = (0 \ 1-i \ 0 \ 1 \ 0 \ 0 \ 0 \ 0 \ -i \ 0 \ 0 \ 0 \ 0 \ 0 \ 0 \ 0), \quad 1.20$$

where the elements of  $I^-$  are found by taking the scalar product of  $I^-$  in Hilbert space with the elements arranged in a row vector, with each basis vector  $U^{(j)}$ . For example:

$$\begin{aligned} I_2^- &= I^- \cdot U^{(2)} \\ &= (0110000100010000) \cdot \frac{1}{2}(0100100000010010) \\ &= \frac{1}{2}(1+1)=1 \end{aligned} \quad 1.21$$

The mean value of  $I^-$  is given by the scalar product:

$$\langle I^- \rangle = I^- \cdot \rho = \rho_2 - i\rho_3 + \rho_5 - i\rho_9 \quad 1.22$$

The elements of the state vector  $\rho$  are found by taking the scalar product of the density matrix in Hilbert space with the basis vectors  $U^{(j)}$ . Thus:

$$\begin{aligned}
\rho_2 = \rho \cdot U^{(2)} &= (\rho_{11}\rho_{12}\rho_{13}\rho_{14}\rho_{21}\rho_{22}\rho_{23}\rho_{24}\rho_{31}\rho_{32}\rho_{33}\rho_{34}\rho_{41}\rho_{42}\rho_{43}\rho_{44}) \cdot \\
&\quad \frac{1}{2}(0 \ 1 \ 0 \ 0 \ 1 \ 0 \ 0 \ 0 \ 0 \ 0 \ 0 \ 1 \ 0 \ 0 \ 1 \ 0) \\
&= \frac{1}{2} (\rho_{12} + \rho_{21} + \rho_{34} + \rho_{43}) \\
\rho_3 = \rho \cdot U^{(3)} &= \frac{1}{2} (-i\rho_{12} + i\rho_{21} - i\rho_{34} + i\rho_{43}) \\
\rho_5 = \rho \cdot U^{(5)} &= \frac{1}{2} (\rho_{13} + \rho_{24} + \rho_{31} + \rho_{42}) \\
\rho_9 = \rho \cdot U^{(9)} &= \frac{1}{2} (-i\rho_{13} - i\rho_{24} + i\rho_{31} + i\rho_{42})
\end{aligned} \tag{1.23}$$

Therefore:

$$\begin{aligned}
I^- \cdot \rho &= \frac{1}{2}(\rho_{12} + \rho_{21} + \rho_{34} + \rho_{43}) - \frac{1}{2}i (-i\rho_{12} + i\rho_{21} - i\rho_{34} + i\rho_{43}) \\
&\quad + \frac{1}{2}(\rho_{13} + \rho_{24} + \rho_{31} + \rho_{42}) - \frac{1}{2}i (-i\rho_{13} - i\rho_{24} + i\rho_{31} + i\rho_{42}) \\
&= \rho_{21} + \rho_{43} + \rho_{31} + \rho_{42}
\end{aligned} \tag{1.24}$$

This result is equivalent to that found by taking the trace of  $(I^- \rho)$ . (see equation 1.17)

The elements of the state vector, required for evaluating the mean value of an operator, are found explicitly by solving the equation of motion. In Hilbert space, the equation of motion of the density matrix is given by:

$$d\rho/dt = -i\hbar^{-1} (H\rho - \rho H), \tag{1.25}$$

where  $H$  is the Hamiltonian operator.

Since this equation conserves the value of  $\text{Tr}(\rho^2)$  where  $r \gg 1$ , it conserves the length of  $\rho$  which is  $\text{Tr}(\rho^2)$  and

therefore represents an infinitesimal rotation of the vector space. It can therefore be written as:

$$dp/dt = -iLp, \quad 1.26$$

where the explicit form of L, the Liouville operator, is obtained by comparing equations 1.25 and 1.26:

$$\begin{aligned} L_{mn,m'n'} &= \hbar^{-1} [H_{mm'} \delta_{nn'} - H_{n'n} \delta_{mm'}] \\ &= \hbar^{-1} [H_{mm'} \delta_{nn'} - \delta_{mm'} H_{nn'}^*] \end{aligned} \quad 1.27$$

or more compactly:

$$L = \hbar^{-1} (HE^* - EH^*) \quad 1.28$$

where E is the identity matrix and the operator products are direct products<sup>1</sup>. The solution of the equation of motion will not be discussed here, because in the present application it will be assumed that the time rate of change of the state vector is zero so that the problem is reduced to that of solving a set of linear equations. The time variation of the state vector in the general case is discussed in reference (13).

---

1. See Appendix 1 for the definition of a direct product.

## C. Derivation of the Lineshape Equation

### I. The State Vector

The state of a system in quantum mechanics is represented, in a finite Hilbert space, by a density matrix(6). The elements of this matrix can be arranged to form a column vector in a suitably defined vector space which we call the Liouville space. If the system of interest consists of a large number of molecules with identical Hamiltonians, the density matrix is given by the ensemble average of the density matrix for an individual molecule. The state vector of such a system is called a primitive state vector and the corresponding vector space a primitive Liouville space. The dimension of the space is  $2^{2n_k}$  where  $n_k$  is the number of spin  $\frac{1}{2}$  nuclei in each molecule. Thus the state vector for an AB spin system is composed of 16 elements. For a system containing several types of molecules, the density matrix of the complete system is given by the direct product of the individual density matrices and the state vector is specified in the interaction Liouville space of dimension  $\prod_k 2^{2n_k}$ . For example, to look at the behavior of an AB spin system undergoing exchange between two different configurations, the complete density matrix of the system would be given by  $\rho = \rho^I \otimes \rho^{II}$  where the elements of  $\rho$  are:

$$\rho_{ij,kl} = \rho_{ik}^I \rho_{jl}^{II}$$



It seems, therefore, that even for the simple problem of an exchanging two-spin system, the state vector consists of 256 elements. We can, however, greatly reduce the dimensionality of the problem by making the assumption that the state vector can be constructed from the components of a vector  $\rho^c$  in composite Liouville space and of a vector  $\rho^b$  depending on all the remaining variables of the system ("bath"). The elements of the composite state vector,  $\rho^c$ , are defined as the renormalized elements of the constituent primitive state vectors, where the renormalization factors are the respective fractional populations  $p_k$  when each type of subsystem contains the same number of nuclei. Thus the dimension of the composite Liouville space, instead of being the product, is simply the sum of the dimensions of the individual primitive state vectors,  $\sum_k 2^{2n_k}$ . For an exchanging two spin system, this means a reduction to 32 from 256. It has been shown (14) that for conditions of "short memory", implying that a molecule remains correlated in time with its neighbours for only short periods, the interaction of the system of interest with the bath can be accounted for by including a dissipative term in the equation of motion of the state vector.

## II. Equation of Motion

The equation of motion of the density matrix in the Hilbert space representation of quantum mechanics is given by:

$$d\rho/dt = -2\pi i [H, \rho] \quad 1.30$$

where H is the high resolution spin Hamiltonian expressed in frequency units (that is, set  $\hbar=1$ ). If we interpret the elements of  $\rho$  as components of a state vector in Liouville space, the equation of motion can be written as:

$$d\rho /dt = -iL\rho \quad 1.31$$

where the elements of the Liouville operator are defined, by correspondence with equation 1.30, as:

$$L_{\mu\nu, \kappa\lambda} = 2\pi [H_{\mu\kappa} \delta_{\nu\lambda} - H_{\lambda\nu} \delta_{\kappa\mu}] \quad 1.32$$

This can be written more compactly as:

$$L = 2\pi [HE^* - EH^*] \quad 1.33$$

where E refers to the identity matrix and the products between matrices are direct products.

In order to account for relaxation processes, (i.e., weak correlations) we include a relaxation operator, R, in

the equation of motion. Similarly, strong correlations, such as slow exchange processes are included under the exchange operator  $\chi$ , so that the equation of motion becomes:

$$d\rho/dt = (-iL+R+\chi)\rho \quad 1.34$$

The representation of the exchange operator  $\chi$  in the composite Liouville space is derived from the equations of Alexander (10) and can be shown to be<sup>1</sup>:

$$\chi_{\mu_r \nu_r, \kappa_s \lambda_s} = \delta_{\mu\kappa} \delta_{\nu\lambda} [-\delta_{rs} \sum_{t(\neq r)} K_{rt} + (1-\delta_{rs}) K_{sr}] \quad 1.35$$

for intramolecular exchange between the magnetic environments  $r$  and  $s$ .

If the relaxation behavior of the system can be approximated by a single transverse relaxation time  $T_2$ , then the relaxation operator  $R$  is diagonal in the representation of the spin product basis functions (16) and all its elements are identical. This approximation is valid in NMR when dealing with solutions of low viscosity and low concentrations. In practice, however, we must account for field-inhomogeneity broadening by including a term  $T_2'$  and using an effective transverse relaxation time  $T_2^{\text{eff}}$  given by:

$$T_2^{\text{eff}} = T_2 T_2' / (T_2 + T_2') \quad 1.36$$

---

1. In order to preserve the continuity of the discussion, the detailed derivation of the exchange operator for a two spin system appears in the appendix.

It now remains to discuss the form of the Liouville operator,  $L$ , appearing in the equation of motion of the state vector. We will do this by using as an illustrative example a two spin system undergoing intramolecular exchange between two configurations, such as the tetra-substituted ethane mentioned in the introduction.

### III. The Liouville Operator

The Liouville operator is given by(13):

$$L = 2\pi[HE^*-EH^*] \quad 1.37$$

where H is the high resolution spin Hamiltonian. If the nuclei of the system of interest are characterized by chemical shifts  $\nu_i^k$  and indirect spin-spin coupling constants,  $J_{ij}^k$ , in Hz, where the superscript k refers to the configuration, then the Hamiltonian  $H^k$  takes the form (16):

$$H^k = H^{ok} + H^{lk} + H^{(t)k} \quad 1.38$$

where:  $H^{ok} = -\sum_i (\nu_i^k - \nu) I_{zi}$  1.39a

$$H^{lk} = \sum_{i < j} J_{ij}^k \underline{I}_i \cdot \underline{I}_j \quad 1.39b$$

$$H^{(t)k} = \frac{\gamma}{2\pi} H_1 \sum_i I_{xi} \quad 1.39c$$

The operators used in equations 1.39 are defined as:

$$I_x |\alpha\rangle = \frac{1}{2} |\beta\rangle; \quad I_x |\beta\rangle = \frac{1}{2} |\alpha\rangle$$

$$I_y |\alpha\rangle = \frac{1}{2} i |\beta\rangle; \quad I_y |\beta\rangle = -\frac{1}{2} i |\alpha\rangle$$

$$I_z |\alpha\rangle = \frac{1}{2} |\alpha\rangle; \quad I_z |\beta\rangle = -\frac{1}{2} |\beta\rangle$$

and  $\underline{I} = I_x \underline{i} + I_y \underline{j} + I_z \underline{k}$

The equations 1.39 hold in a reference frame rotating with angular frequency  $\omega = 2\pi\nu$  in the xy plane relative to the

laboratory frame, so that the time dependence of the radio-frequency field  $H_1$  vanishes and the field is oriented along the x axis. We will choose as our representation for the Hamiltonian the one in which the Zeeman interaction term is diagonal. Thus it suffices to use as the basis set the spin product functions  $\alpha\alpha, \alpha\beta, \beta\alpha,$  and  $\beta\beta$ .

In this basis the representations of the three parts of the spin Hamiltonian are(17):

$$H^0k = \begin{bmatrix} \Delta^k & 0 & 0 & 0 \\ 0 & \frac{1}{2}\delta^k & 0 & 0 \\ 0 & 0 & -\frac{1}{2}\delta^k & 0 \\ 0 & 0 & 0 & -\Delta^k \end{bmatrix}, \text{ where we have used the identities}$$

$$\Delta^k \equiv \nu - \frac{1}{2}(\nu_1^k + \nu_2^k)$$

$$\delta^k \equiv \nu_2^k - \nu_1^k$$

$$H^1k = \begin{bmatrix} \frac{1}{4}J_{12}^k & 0 & 0 & 0 \\ 0 & -\frac{1}{4}J_{12}^k & \frac{1}{2}J_{12}^k & 0 \\ 0 & \frac{1}{2}J_{12}^k & -\frac{1}{4}J_{12}^k & 0 \\ 0 & 0 & 0 & \frac{1}{4}J_{12}^k \end{bmatrix}$$

$$H(t)k = \frac{\gamma}{2} H_1 \begin{bmatrix} 0 & 1 & 1 & 0 \\ 1 & 0 & 0 & 1 \\ 1 & 0 & 0 & 1 \\ 0 & 1 & 1 & 0 \end{bmatrix}$$

where  $\gamma = \frac{\gamma}{2\pi}$

Rewrite the Liouville operator<sup>1</sup> as:

$$L^k = 2\pi [(H^{ok}_{E-EH^{ok}}) + (H^{lk}_{E-EH^{lk}}) + (H^{(t)k}_{E-EH^{(t)k}})]$$

and define:

$$L^{ok} = 2\pi (H^{ok}_{E-EH^{ok}} + H^{lk}_{E-EH^{lk}}) \quad 1.41a$$

and

$$L'^k = 2\pi (H^{(t)k}_{E-EH^{(t)k}}) \quad 1.41b$$

which allows us to write the equation of motion as:

$$d\rho/dt = (-L^o - iL' + R + \chi)\rho \quad 1.42$$

---

1. The symbol \* for complex conjugates is omitted in the following equations because all the elements of L are real.

#### IV. The Steady-State Condition

Under steady-state conditions, which implies slow passage, the time dependence of the state vector vanishes (16), and equation 1.42 becomes:

$$(-iL^0 + R + \chi)\rho = iL^1 \rho \quad 1.43$$

In calculating the right hand side of this equation we can use Alexander's approximation (9) regarding the effect of  $H^{(t)}$  on the density matrix. Because the radio-frequency field  $H_1$  is very small compared to the static field  $H_0$ , the off-diagonal elements of  $\rho$  will be much smaller than the diagonal elements. Thus any product involving  $H_1$  and an off-diagonal element of  $\rho$  will be small enough to be negligible compared to a product involving a diagonal element. Since the diagonal element  $\rho_{mm}$  represents the fractional population of the state  $m$ , the diagonal elements are given by the Boltzmann factors for the corresponding energy levels. In calculating the Boltzmann factors, Whitesides (17) neglects the contribution of the shielding parameters and the coupling constants to the total energy since they are small compared to the contribution of  $H_0$ . Thus we arrive at the approximate representation of the density matrix for an AB spin system:



$$\rho \approx 1/4 \begin{bmatrix} 1 + \gamma H_0 / kT & 0 & 0 & 0 \\ 0 & 1 & 0 & 0 \\ 0 & 0 & 1 & 0 \\ 0 & 0 & 0 & 1 - \gamma H_0 / kT \end{bmatrix} \quad 1.44$$

We will now work out the explicit form of  $L'$ :

$$L' = 2\pi [H^{(t)} E - E H^{(t)}] \quad 1.45$$

Recalling that the products between matrices are direct products, we have:

$$H^{(t)}_{E=\gamma H_1/2} \begin{bmatrix} 0 & 0 & 0 & 0 & 1 & 0 & 0 & 0 & 1 & 0 & 0 & 0 & 0 & 0 & 0 & 0 \\ 0 & 0 & 0 & 0 & 0 & 1 & 0 & 0 & 0 & 1 & 0 & 0 & 0 & 0 & 0 & 0 \\ 0 & 0 & 0 & 0 & 0 & 0 & 1 & 0 & 0 & 0 & 1 & 0 & 0 & 0 & 0 & 0 \\ 0 & 0 & 0 & 0 & 0 & 0 & 0 & 1 & 0 & 0 & 0 & 1 & 0 & 0 & 0 & 0 \\ 1 & 0 & 0 & 0 & 0 & 0 & 0 & 0 & 0 & 0 & 0 & 0 & 1 & 0 & 0 & 0 \\ 0 & 1 & 0 & 0 & 0 & 0 & 0 & 0 & 0 & 0 & 0 & 0 & 0 & 1 & 0 & 0 \\ 0 & 0 & 1 & 0 & 0 & 0 & 0 & 0 & 0 & 0 & 0 & 0 & 0 & 0 & 1 & 0 \\ 0 & 0 & 0 & 1 & 0 & 0 & 0 & 0 & 0 & 0 & 0 & 0 & 0 & 0 & 0 & 1 \\ 1 & 0 & 0 & 0 & 0 & 0 & 0 & 0 & 0 & 0 & 0 & 0 & 1 & 0 & 0 & 0 \\ 0 & 1 & 0 & 0 & 0 & 0 & 0 & 0 & 0 & 0 & 0 & 0 & 0 & 1 & 0 & 0 \\ 0 & 0 & 1 & 0 & 0 & 0 & 0 & 0 & 0 & 0 & 0 & 0 & 0 & 0 & 1 & 0 \\ 0 & 0 & 0 & 1 & 0 & 0 & 0 & 0 & 0 & 0 & 0 & 0 & 0 & 0 & 0 & 1 \\ 0 & 0 & 0 & 0 & 1 & 0 & 0 & 0 & 1 & 0 & 0 & 0 & 0 & 0 & 0 & 0 \\ 0 & 0 & 0 & 0 & 0 & 1 & 0 & 0 & 0 & 1 & 0 & 0 & 0 & 0 & 0 & 0 \\ 0 & 0 & 0 & 0 & 0 & 0 & 1 & 0 & 0 & 0 & 1 & 0 & 0 & 0 & 0 & 0 \\ 0 & 0 & 0 & 0 & 0 & 0 & 0 & 1 & 0 & 0 & 0 & 1 & 0 & 0 & 0 & 0 \end{bmatrix} \quad 1.46$$



$$iL'\rho = \frac{i\gamma H_1 \cdot \frac{1}{4}}{2} \begin{bmatrix} 0110 & 1000 & 1000 & 0000 \\ 1001 & 0100 & 0100 & 0000 \\ 1001 & 0010 & 0010 & 0000 \\ 0110 & 0001 & 0001 & 0000 \\ \\ 1000 & 0110 & 0000 & 1000 \\ 0100 & 1001 & 0000 & 0100 \\ 0010 & 1001 & 0000 & 0010 \\ 0001 & 0110 & 0000 & 0001 \\ \\ 1000 & 0000 & 0110 & 1000 \\ 0100 & 0000 & 1001 & 0100 \\ 0010 & 0000 & 1001 & 0010 \\ 0001 & 0000 & 0110 & 0001 \\ \\ 0000 & 1000 & 1000 & 0110 \\ 0000 & 0100 & 0100 & 1001 \\ 0000 & 0010 & 0010 & 1001 \\ 0000 & 0001 & 0001 & 0110 \end{bmatrix} \begin{bmatrix} 1+\gamma H_0/kT \\ 0 \\ 0 \\ 0 \\ \\ 0 \\ 1 \\ 0 \\ 0 \\ \\ 0 \\ 0 \\ 1 \\ 0 \\ \\ 0 \\ 0 \\ 0 \\ 1-\gamma H_0/kT \end{bmatrix} = \frac{i\gamma H_1 \cdot \frac{1}{4}}{2} \begin{bmatrix} 0 \\ -\gamma H_0/kT \\ -\gamma H_0/kT \\ 0 \\ H_0/kT \\ 0 \\ 0 \\ -\gamma H_0/kT \\ H_0/kT \\ 0 \\ 0 \\ -\gamma H_0/kT \\ 0 \\ \gamma H_0/kT \\ \gamma H_0/kT \\ 0 \end{bmatrix}$$

1.49

If  $C = \frac{\gamma^2 H_1 H_0}{16\hbar kT}$ , then

$$iL'\rho = iC \begin{bmatrix} 0 \\ -1 \\ -1 \\ 0 \\ 1 \\ 0 \\ 0 \\ -1 \\ 1 \\ 0 \\ 0 \\ -1 \\ 0 \\ 1 \\ 1 \\ 0 \end{bmatrix} = iC\sigma \quad 1.50$$

The above equation accounts for only one of the configurations of the AB spin system, so that for the total system  $iL'\rho$  would have twice as many elements, but the last sixteen would be identical to the first sixteen, except that we would multiply each of the two parts by the corresponding

fractional populations. If the populations are equal, then the factor  $\frac{1}{2}$  can be absorbed into the constant C.

Equation 1.50 can be written more compactly as:

$$\sigma_{\mu\nu}^k = U_{\mu\nu} (F_Z^{\nu} - F_Z^{\mu}) p^k, \quad 1.51$$

where  $U_{\mu\nu}$  is equal to 1 if  $\mu$  and  $\nu$  refer to spin basis functions that differ by precisely one individual spin z component  $I_z$ , and zero otherwise,  $F_Z = \sum_i I_{zi}$ , and  $p^k$  is the fractional population of configuration k.

Making use of equations 1.40 we can calculate  $L^{ok}$  in a manner analogous to that used for finding  $L'$ :

$L^0 =$

11	12	13	14	21	22	23	24	31	32	33	34	41	42	43	44
0	0	0	0												
0	$\Delta - \frac{1}{2}\delta + \frac{J}{2}$	$-\frac{J}{2}$	0												
0	$-\frac{J}{2}$	$\Delta + \frac{1}{2}\delta + \frac{J}{2}$	0												
0	0	0	$2\Delta$												
				$\frac{1}{2}\delta - \Delta - \frac{J}{2}$	0	0	0	$+\frac{J}{2}$	0	0	0				
				0	0	$-\frac{J}{2}$	0	0	$+\frac{J}{2}$	0	0				
				0	$-\frac{J}{2}$	$\frac{1}{2}\delta + \frac{1}{2}\delta$	0	0	0	$+\frac{J}{2}$	0				
				0	0	0	$\frac{1}{2}\delta + \Delta - \frac{J}{2}$	0	0	0	$+\frac{J}{2}$				
				$+\frac{J}{2}$	0	0	0	$-\frac{1}{2}\delta - \Delta - \frac{J}{2}$	0	0	0				
				0	$+\frac{J}{2}$	0	0	0	$-\frac{1}{2}\delta - \frac{1}{2}\delta$	$-\frac{J}{2}$	0				
				0	0	$+\frac{J}{2}$	0	0	$-\frac{J}{2}$	0	0				
				0	0	0	$+\frac{J}{2}$	0	0	0	$-\frac{1}{2}\delta + \Delta - \frac{J}{2}$				
												$-2\Delta$	0	0	0
												0	$-\Delta - \frac{1}{2}\delta + \frac{J}{2}$	$-\frac{J}{2}$	0
												0	$-\frac{J}{2}$	$-\Delta + \frac{1}{2}\delta + \frac{J}{2}$	0
												0	0	0	0

Upon defining the complex non-hermitian operator  $M_0$  as

$$M_0 = -iL^0 + R + X \quad 1.53$$

equation 1.43 can be rewritten as

$$M_0 \rho = iL^0 \rho = iC\sigma \quad 1.54$$

Assuming that  $M_0$  has an inverse, the solution of this equation is given by:

$$\rho = iCM_0^{-1}\sigma \quad 1.55$$

In high-resolution N.M.R. one is interested in the complex magnetization in the xy plane, which is given by the mean value of the operator  $I^-$ . In the Liouville representation the mean value of an operator is given by its scalar product with the state vector  $\rho$ :

$$\langle I^- \rangle = I^- \cdot \rho = iCI^-M_0^{-1}\sigma \quad 1.56$$

In the basis of the spin product functions, the representation of the operator  $I^-$  in Hilbert space is:

$$I^- = \begin{bmatrix} 0 & 1 & 1 & 0 \\ 0 & 0 & 0 & 1 \\ 0 & 0 & 0 & 1 \\ 0 & 0 & 0 & 0 \end{bmatrix} \quad 1.57$$

Since this is the same for both configurations of the AB spin system,  $I^-$  in the composite Liouville space is the row vector:

$$I^- = (01100001000100000110000100010000) \quad 1.58$$

It is seen that many elements of the  $I^-$  row vector vanish, so that it represents a projection of  $\rho$  from the composite Liouville space into a smaller subspace. The non vanishing elements of  $I^-$  are those for which  $\Delta F_z = -1$ , where  $F_z = \sum_i I_{zi}$ . Examination of the  $L^0$  matrix shows that it does not cause mixing between those elements of  $\rho$  which obey this selection rule and those which do not, so that the solution to the problem may be formulated in a contracted subspace. By adding the necessary terms from the exchange operator  $\chi$ , (found in the appendix) and the relaxation operator  $R$ , which is assumed to be diagonal, the contracted  $M_0$  matrix for the spin system under consideration becomes:

$M_0 =$

	$12^I$	$13^I$	$24^I$	$34^I$	$12^{II}$	$13^{II}$	$24^{II}$	$34^{II}$
$12^I$	$-2\pi i(\Delta^I - \frac{1}{2}\delta^I + \frac{J^I}{2})$ $-\frac{1}{T_2} - K_{12}$	$i\pi J^I$			$K_{21}$			
$13^I$	$i\pi J^I$	$-2\pi i(\Delta^I + \frac{1}{2}\delta^I + \frac{J^I}{2})$ $-\frac{1}{T_2} - K_{12}$				$K_{21}$		
$24^I$			$-2\pi i(\Delta^I + \frac{1}{2}\delta^I - \frac{J^I}{2})$ $-\frac{1}{T_2} - K_{12}$	$-i\pi J^I$			$K_{21}$	
$34^I$			$-i\pi J^I$	$-2\pi i(\Delta^I - \frac{1}{2}\delta^I - \frac{J^I}{2})$ $-\frac{1}{T_2} - K_{12}$				$K_{21}$
$12^{II}$	$K_{12}$				$-\frac{1}{T_2} - K_{21}$	$i\pi J^{II}$		
$13^{II}$		$K_{12}$			$i\pi J^{II}$	$-2\pi i(\Delta^{II} + \frac{1}{2}\delta^{II} + \frac{J^{II}}{2})$ $-\frac{1}{T_2} - K_{21}$		
$24^{II}$			$K_{12}$			$-2\pi i(\Delta^{II} + \frac{1}{2}\delta^{II} - \frac{J^{II}}{2})$ $-\frac{1}{T_2} - K_{21}$	$-i\pi J^{II}$	
$34^{II}$				$K_{12}$		$-i\pi J^{II}$		$-2\pi i(\Delta^{II} - \frac{1}{2}\delta^{II} - \frac{J^{II}}{2})$ $-\frac{1}{T_2} - K_{21}$



The line shape equation 1.56 in the contracted Liouville subspace is then

$$\langle I^- \rangle = i \tilde{C} \tilde{I}^{-1} \tilde{M}_0^{-1} \tilde{\sigma} = -i \tilde{C} \tilde{I}^{-1} \tilde{M}_0 P \quad 1.60$$

where the tilde indicates that the quantities referred to are now given in the contracted subspace and the elements of P are the fractional populations of the corresponding configurations. The absorption lineshape function is extracted from this equation as the imaginary part of  $\langle I^- \rangle$ , or equivalent to this, the negative real part of  $i \langle I^- \rangle$ :

$$Y = -C \operatorname{Re} [\tilde{I}^{-1} \tilde{M}_0^{-1} P] \quad 1.61$$

All the quantities on the right hand side of this equation are known and the only computational difficulty is encountered in finding the inverse of the matrix  $M_0$ . An efficient method for doing this is outlined in the next section.

#### D. Computational Procedure

It was found in the last section that a line-shape calculation involves the inversion of the complex non-Hermitian matrix  $M_0$  for each point of the spectrum.

Since matrix inversion is a time consuming process, use of the line-shape equation in the given form is impractical so that some simplification of it seems desirable.

Inspection of the form of the  $M_0$  matrix reveals that the radio-frequency dependence,  $\nu$ , appears only in the diagonal elements, so that the matrix can be written as a sum of two matrices:

$$M_0 = B - 2\pi i \nu E \quad 1.62$$

where  $E$  is the identity matrix and the matrix  $B$  contains only elements which are independent of the radio-frequency and hence is the same for all points of the spectrum.

In general, for any nonsingular matrix there exists a similarity transformation  $U$  so that

$$U^{-1} M_0 U = D \quad 1.63$$

where  $D$  will always be an upper or lower triangular matrix. Furthermore, it is assumed by Binsch (14) that in all practical application of the theory under consideration  $D$  will turn out to be diagonal.<sup>1</sup>

---

1. However, this is not true in general. Pathological cases can be constructed artificially, although they are rare in practical applications. Diagonalization by this procedure is not possible in the presence of extensive degeneracies. The computer program DNMR will detect such a case and reject it.

Because the identity matrix  $E$  commutes with all matrices, it will commute with  $B$ , so that the transformation matrix which diagonalizes  $M_0$  will also diagonalize  $B$ . One obtains:

$$\begin{aligned} U^{-1}M_0U &= U^{-1}BU - 2\text{Hiv}U^{-1}EU & 1.64 \\ &= \Lambda - 2\text{Hiv}E = D \end{aligned}$$

Multiplying both sides of this equation by  $U$  from the left and  $U^{-1}$  from the right one arrives at:

$$UU^{-1}M_0UU^{-1} = M_0 = U(\Lambda - 2\text{Hiv}E)U^{-1} = UDU^{-1} \quad 1.65$$

The expression for  $M_0^{-1}$  then becomes:

$$M_0^{-1} = U(\Lambda - 2\text{Hiv}E)^{-1}U^{-1} = UD^{-1}U^{-1} \quad 1.66$$

The expressions on the right hand side follow from the matrix identity:

$$(XY)^{-1} = Y^{-1}X^{-1}$$

From the foregoing discussion it follows that the only nontrivial step in the computational procedure is the finding of the eigenvalues and eigenvectors of the matrix  $B$ . The eigenvalues become the elements of the matrix  $\Lambda$  and the eigenvectors form the columns of the matrix  $U$ , which is then inverted to form  $U^{-1}$ . This step, however, has to be carried out only once for each spectrum,

so that the calculation of the individual points involves only the inversion of the diagonal matrix D and two matrix multiplications. - Substituting the expression for  $M_0^{-1}$  from equation 1.66 into the line-shape equation 1.61, one obtains:

$$Y = -\text{Re} [C I^{-1} U (\Lambda - 2\pi i \nu E)^{-1} U^{-1} P] \quad 1.67$$

We define a "spectral vector" Q by the elements:

$$Q_\mu = (\Lambda_{\mu\mu} - 2\pi i \nu)^{-1} \quad 1.68$$

Using the definition of matrix multiplication, the following expression for Y is obtained:

$$Y = -\text{Re} [C \sum_\lambda I_\lambda^{-1} \sum_\mu U_{\lambda\mu} Q_\mu \sum_\nu U_{\mu\nu}^{-1} P_\nu] \quad 1.69$$

It is possible to separate out the radio-frequency independent part of this equation by defining a "shape vector", S, by the elements:

$$S_\mu = \sum_\lambda I_\lambda^{-1} U_{\lambda\mu} U_{\mu\nu}^{-1} P_\nu \quad 1.70$$

This allows one to formulate the absorption line-shape as the negative real part of the scalar product of two vectors multiplied by the constant C:

$$Y = -C \text{Re}(Q \cdot S) \quad 1.71$$

The computer program, DNMR, written by G.Binsch and D.A.Kleier(18) makes use of the method outlined above to calculate line shapes for exchanging spin systems. In its present form it is limited to systems of spin  $\frac{1}{2}$  nuclei and is capable of handling a spin system whose contracted  $M_0$  matrix is not larger than  $48 \times 48$ . This means that it can treat four-spin systems exchanging between two different configurations, or three-spin systems exchanging between three different configurations.

The program, written in FORTRAN IV, consists of nine subroutines in addition to the main program. The following is a brief outline of how the program works:

#### MAIN

The principal purpose of the main program is to call the various subroutines in the required order, thus maintaining a logical flow in the computation. It also reads the rate constants and the scaling parameters required for plotting.

#### STADAT

This subroutine reads and prints the parameters required for calculating the Hamiltonian.

#### BASIS

This subroutine generates the  $2^N$  basis functions for a system of  $N$  spins in the form of binary numbers and computes their  $I_z$  components.

## HAMILT

This subroutine computes the matrix elements of the Hamiltonian for each configuration.

## PROJECT

The vectors  $I^-$  and  $\sigma$  are computed, in addition to three index arrays needed for the projection of the density matrix vector into the proper Liouville subspace.

## PERMUT

This subroutine, called only in cases of mutual exchange, computes the permutation matrix P for each chemical configuration.

## TRAMAT

Here the complex elements of the matrix B are computed and the submatrices are assembled.

## ALLMAT

This subroutine uses an iterative algorithm to find the eigenvalues and eigenvectors of the matrix B.

## NVERT

The eigenvector matrix is inverted here to obtain  $U^{-1}$ .

## CONVEC

This subroutine uses the results of ALLMAT and NVERT to construct the shape vector S and the constant part of the spectral vector Q.

## SPECT

In this subroutine the requested number of points is computed from equation 1.71 and, depending on the value of a control parameter, gives the output as a series of X and Y values, where X is the frequency and Y the corresponding intensity, or calls the subroutine GRAPH.

## GRAPH

This subroutine plots the points obtained in SPECT on the lineprinter or on a Calcomp plotter, depending on which one is requested.

The ordering of the data deck is done in the following way:

card 1:   NRUN,N,NE,MU                                   FORMAT(I3,3I1)

NRUN=nonzero run number

N=number of nuclei

NE=number of chemical configurations

MU=1 for mutual exchange, 0 otherwise

card 2:   TEXT   FORMAT(12A6)

alphanumeric information to be printed on top of output sheet.

If no such information is desired, insert blank card here.

card 3:   (W(I,J), J = 1,N)                             FORMAT(4F10.0)

chemical shifts(in Hz relative to arbitrary reference) for chemical configuration I

card 4: Next set of cards coupling constants (in Hz)  
for chemical configuration I

(AJ(I,J,K),...)                      FORMAT(3F10.0)

first card of this set AJ(I,1,2),AJ(I,1,3),...,  
AJ(I,1,N)

second card of this set AJ(I,2,3),AJ(I,2,4),...,  
AJ(I,2,N) etc.

last card of this set AJ(I,N-1,N)

Note: the labeling of the coupling constants has  
to correspond to the labeling of the chemi-  
cal shifts.

Note: skip set 4 if  $N = 1$

card 5: If MU=0, repeat 3 and 4 for all chemical con-  
figurations I, and then proceed to 7

if MU=1, proceed to 6

card 6: Next set of cards exchange vectors for mutual  
exchange, one per card (IE(I,K),K=1,N)FORMAT(4I1)

first card of this set, second exchange vector

second card of this set, third exchange vector, etc.

The integer elements of the n'th exchange vector  
represent the labeling of the nuclei in the n'th chemi-  
cal configuration in terms of the consecutive labeling  
chosen for the first chemical configuration.



card 7: NRS,LPUNCH,LPRINT,LGRAPH,FR1,FR2,SCALE,HEIGHT,  
DENS,FORMAT(I2,3I1,5X5F10.4)

NRS=number of sets of rate constants

if LPUNCH = 1 the x and y components of the spectra  
are punched out, four sets (i.e. x,y) per card

FORMAT(8F10.4)

if LPUNCH = 0, no punched-card output

If LPRINT = 1,x and y components are printed.

If LPRINT = 0, no output.

FR1 is left plot frequency (in Hz)

FR2 is right plot frequency (in Hz)

DENS = no.points/in.

SCALE is horizontal plotting scale (in mm/Hz)

HEIGHT is height of highest peak in spectrum (in mm),  
limited to 240 mm.

LGRAPH = 1 "\*" output on printer

= 9 calcomp plot

Note: FR1<FR2

card 8: If MU = 0, proceed to 9; if MU = 1, proceed to 10

card 9: (POP(I),I=1,NE) FORMAT(3F10.0)

populations of the chemical configurations

card 10: T2 FORMAT(F10.0)

effective transverse relaxation time (in sec);  $T_2$  is  
related to the width W(in Hz) at half height of single  
peaks not broadened by exchange by  $T_2 = 1/(\pi W)$

card 11: If NE=1, proceed to 14, otherwise proceed to 12

card 12: Next set of cards rate constants RC(I,J) in  
sec<sup>-1</sup>, one per card and HEIGHT(note:HEIGHT can be  
omitted here, if same as in 7)       FORMAT(2F10.0)

card sequence:RC(1,2),RC(1,3),...,RC(1,NE),RC(2,3),  
                  ...,RC(NE-1,NE)

Note: for MU=1, this set consists of a single card  
only, with RC(1,2), regardless of the number of  
chemical configurations

card 13: Repeat 12 for all (NRS) sets of rate constants

card 14: Next problem follows, repeat 1 through 13

card 15: After last problem blank card

CHAPTER III

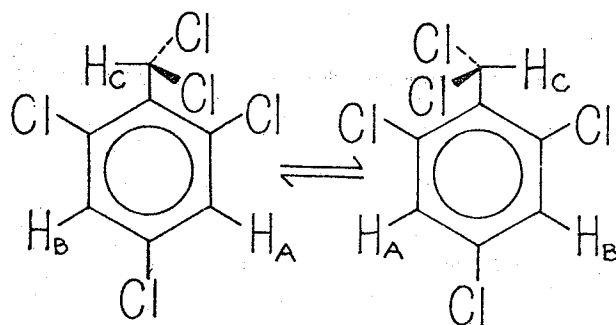
APPLICATION OF THE THEORY TO AN ABC SPIN SYSTEM

## A. Introduction

The theory discussed in the previous chapter is applied to the rate process involved in the hindered rotation of the methyl group in the molecule  $\alpha,\alpha,2,4,6$ -pentachlorotoluene. The proton magnetic resonance spectrum of this molecule changes with temperature from a well defined ABC below  $-30^{\circ}\text{C}$ , through a series of gradually broadened lines as the temperature is raised, to an  $A_2B$  spectrum above  $70^{\circ}\text{C}$ . This gradual change in the line-shape indicates that a rate process is taking place in which two of the protons are exchanging sites. At low temperatures the lifetime of each proton in a given site is long enough to allow detection of the individual chemical shifts. At very high temperatures, where the exchange rate is much higher than the frequency separation between the two sites, the exchanging protons are observed to experience an average of the two chemical environments. The change in the line-shape as a function of temperature is illustrated in Figure 1 which shows the spectrum at  $-34^{\circ}\text{C}$ , where the exchange rate is very small, at  $30^{\circ}\text{C}$  where the individual lines have coalesced, and at  $72^{\circ}\text{C}$  where the lines have sharpened up again but the exchanging protons exhibit identical chemical shifts.

The observed rate process is due to the hindered

rotation of the dichloromethyl group, which gives rise to the two configurations:



The above labeling of protons will be maintained throughout this chapter. It is seen that the rotation of the methyl group causes the environments of protons  $H_A$  and  $H_B$  to interchange, while the environment of proton  $H_C$  remains unchanged. For this reason the resonance lines due to  $H_C$  remain sharp throughout the entire temperature range, but change from a doublet, due to coupling with  $H_A$  at low temperature, to a triplet at high temperature where it is coupled virtually equally to  $H_A$  and  $H_B$ . The symmetry of the molecule requires that the two sites be equally populated, so that the rotation is governed by a single rate constant.

The following section of this chapter deals with the method of obtaining all the parameters required for calculating the rate constants. These include the chemical shifts, the coupling constants, and the effective transverse relaxation times at each temperature. In the third

section the procedure for obtaining the rate constants is described, while the final section is concerned with the calculation of the thermodynamic parameters for the rotation.

## B. Experimental Procedure and Analysis of Spectra

The compound,  $\alpha,\alpha,2,4,6$ -pentachlorotoluene, was prepared as described by Fuhr (19). A 15 mole % solution of this compound in  $\text{CS}_2$  was prepared, with tetramethylsilane (TMS) used as an internal reference. These chemicals were obtained from Matheson, Coleman and Bell and Chem. Service, respectively.

The proton magnetic resonance spectra were obtained on a Varian DA-60 I Spectrometer equipped with a Varian-4343 variable temperature controller. Four spectra were recorded at each temperature studied, and the exact temperature ( $\pm 1^\circ\text{C}$ ) was determined in each case from the temperature dependence of the internal chemical shift of the protons in ethylene glycol (at high temperatures) or methanol (at low temperatures). The spectra were recorded at a sweep rate of 0.02 Hz/sec and the calibrations were done by the period-averaging technique.

The spectrum of  $\alpha,\alpha,2,4,6$ -pentachlorotoluene at  $-34^\circ\text{C}$  is shown in Figure 1 and is seen to consist of a quartet and two doublets. The lines marked with an x in the figure are due to impurities, the prominent one arising from  $\alpha,\alpha,\alpha,2,4,6$ -hexachlorotoluene. The doublet to low field was assigned to the sidechain proton  $\text{H}_C$ , the quartet to the ring proton  $\text{H}_A$ , and the slightly broadened doublet

FIGURE 1

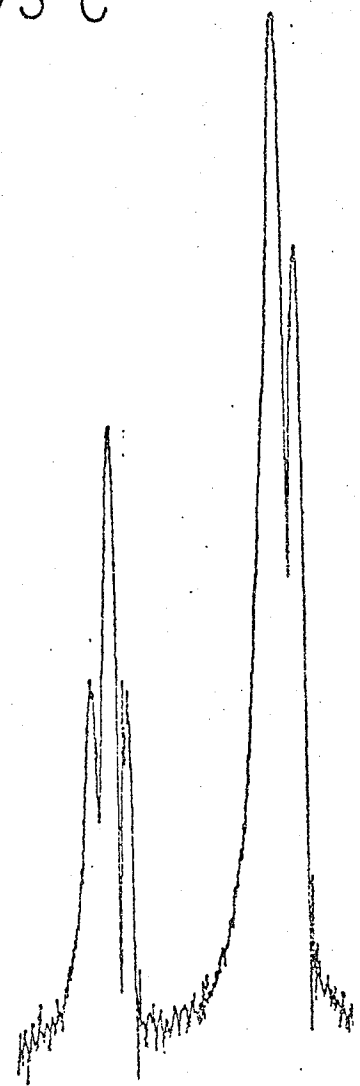
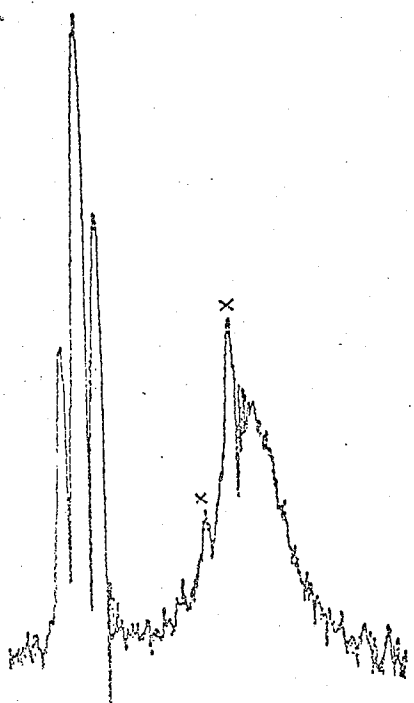
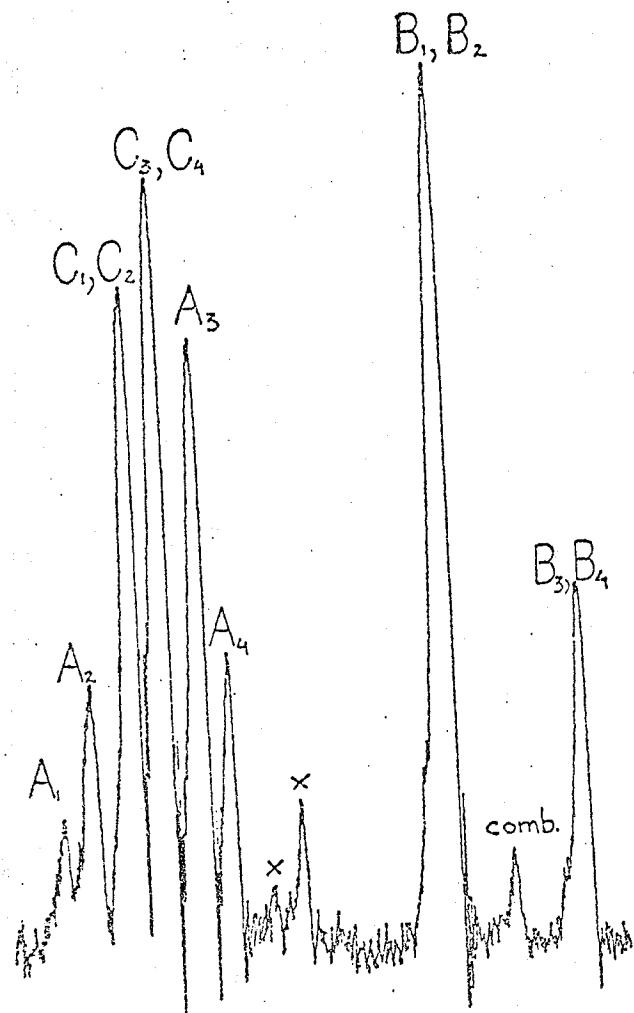
The proton magnetic resonance spectrum of  $\alpha,\alpha,2,4,6$ -pentachlorotoluene at  $-34^{\circ}\text{C}$ ,  $30^{\circ}\text{C}$ , and  $73^{\circ}\text{C}$ . The resonance lines marked with an x are due to impurities.



-34°C

30°C

73°C



to high field was assigned to the other ring proton  $H_B$ . This assignment was made on the basis that the largest coupling occurs between the two ring protons and that, according to the zig-zag rule (20),  $H_C$  is coupled to  $H_A$  but not to  $H_B$ . The slight broadening of the  $H_B$  doublet is probably due to an unresolved coupling to  $H_C$ . On the basis of these assignments several low temperature spectra were analyzed, using the computer program LAOCN3(37), in order to find the temperature dependence of the chemical shifts and coupling constants. However, as seen in Table 1, the variation of these parameters with temperature is too small to indicate a definite trend. The internal shift  $\nu_{AB}$  was constant to within 0.2Hz in the temperature range  $-65^\circ\text{C}$  to  $-34^\circ\text{C}$ . This parameter will have the largest effect on the line-shape because it is this shift which is averaged by the exchange process. In the initial calculation of the theoretical spectra, the shift and coupling parameters used were those found by analysis of the experimental spectrum at  $-34^\circ\text{C}$ . To obtain the best fits, however, it was found necessary to alter some of the shift parameters by as much as 0.5Hz, but the coupling constants and the internal shift  $\nu_{AB}$  were held constant in all line-shape calculations.

The effective transverse relaxation times,  $T_2^{\text{eff}}$ , were calculated at each temperature from the half-height line-widths of the impurity peak due to  $\alpha,\alpha,\alpha,2,4,6-$

TABLE 1

Chemical shifts<sup>†</sup> and coupling constants\* of some low temperature spectra as analysed by LAOCN3

Temperature <u>°C</u>	<u><math>\nu_A</math></u>	<u><math>\nu_B</math></u>	<u><math>\nu_C</math></u>	<u><math>J_{AB}</math></u>	<u><math>J_{AC}</math></u>	<u><math>J_{BC}</math></u>
-65°	440.10	434.58	440.75	2.12	0.52	0.13
-61°	440.14	434.54	440.71	2.15	0.49	0.10
-58°	439.90	434.51	440.58	2.16	0.53	0.11
-50°	440.44	434.81	440.71	2.15	0.51	0.10
-40°	440.52	434.95	440.71	2.18	0.44	0.07
-34°	440.68	435.11	440.82	2.14	0.50	0.10

<sup>†</sup> In Hz, at 60 MHz, to low field of tetramethylsilane; probable errors do not exceed 0.02 Hz.

\* In Hz; probable errors do not exceed 0.03Hz.

hexachlorotoluene, using the relation:

$$T_2^{\text{eff}} = \frac{1}{\Pi v_{1/2}}, \quad 2.1$$

where  $v_{1/2}$  is the linewidth at half height measured in Hz.

The input parameters used in the final calculations are summarized in Table 2.

TABLE 2

The static parameters used in calculating the lineshapes.

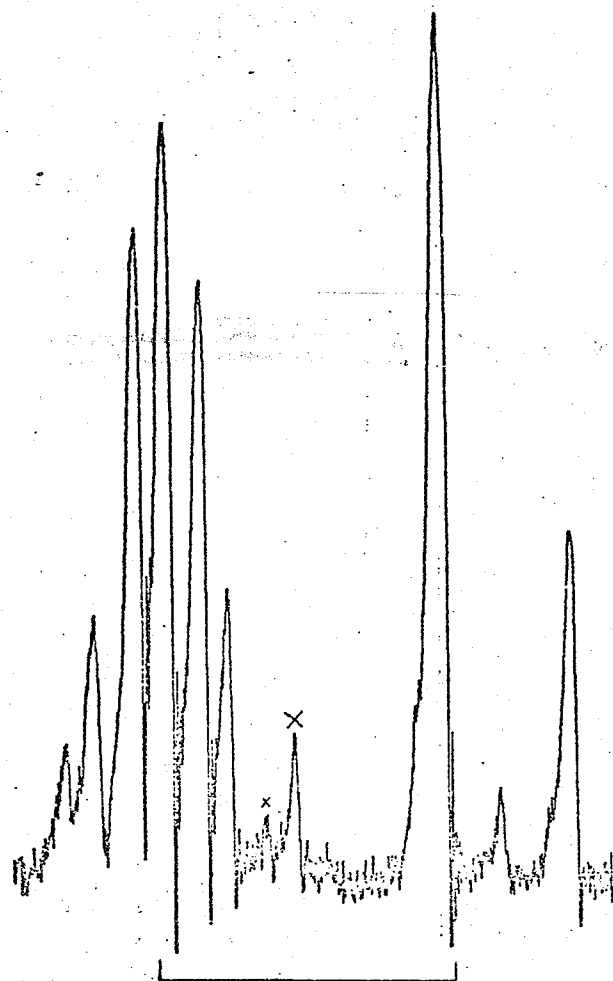
Temperature (°C)	$\nu_A$ (Hz)	$\nu_B$ (Hz)	$\nu_C$ (Hz)	$J_{AB}$ (Hz)	$J_{AC}$ (Hz)	$J_{BC}$ (Hz)	$T_2^{eff}$ (sec)
-34	440.69	435.11	440.82	2.15	0.51	0.12	1.38
-15	440.95	435.37	440.85	2.15	0.51	0.12	1.38
0	441.26	435.65	441.22	2.15	0.51	0.12	1.52
10	441.39	435.81	441.20	2.15	0.51	0.12	1.87
18	441.08	435.11	440.82	2.15	0.51	0.12	2.80
30	441.28	435.70	441.20	2.15	0.51	0.12	1.90
47	441.14	435.56	441.15	2.15	0.51	0.12	1.90
62	441.11	435.53	441.09	2.15	0.51	0.12	1.5
73	441.16	435.58	441.13	2.15	0.51	0.12	1.5

### C. Calculation of the Rate Constants

Theoretical line-shape calculations were done using the computer program DNMR which is described in the last section of Chapter II. All computations were carried out on an IBM 360/65 computer. A large number of calculated spectra with various rate constants were plotted on a Calcomp plotter and were compared visually with the experimental spectra. The scale used in plotting was 1Hz/cm to correspond with the recorded spectra. The density of points was 100/in. Each spectrum spanned twenty-five Hz and therefore consisted of approximately 1000 points. The computational time required for one spectrum is approximately 1 minute execution time and 4.66 sec. CPU time. This is quite economical compared to other methods (21) of calculation. Furthermore, increasing the number of points per spectrum would cause very little increase in computer time as is evident from the discussion in Chapter II. The experimental spectra at nine temperatures and the calculated spectra with the corresponding rate constants are shown in Figures 2-10. Quite good fits were obtained for the spectra at intermediate rates of exchange because in this region the line-shape is very sensitive to the rate constant, but at the two extremes of slow and fast exchange the spectrum depends largely on

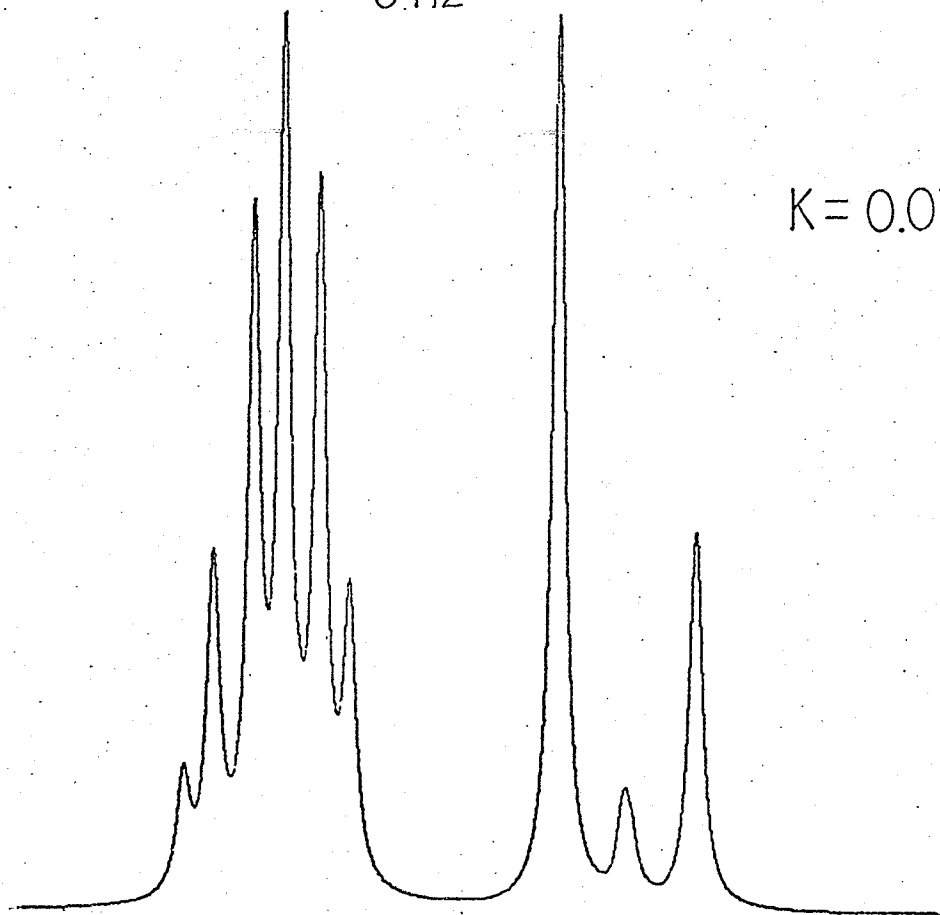
FIGURE 2

Experimental spectrum at  $-34^{\circ}\text{C}$  and the  
corresponding calculated spectrum.



$T = -34^{\circ}\text{C}$

5 Hz



$K = 0.075 \text{ SEC}^{-1}$



FIGURE 3

Experimental spectrum at  $-15^{\circ}\text{C}$  and the  
corresponding calculated spectrum.

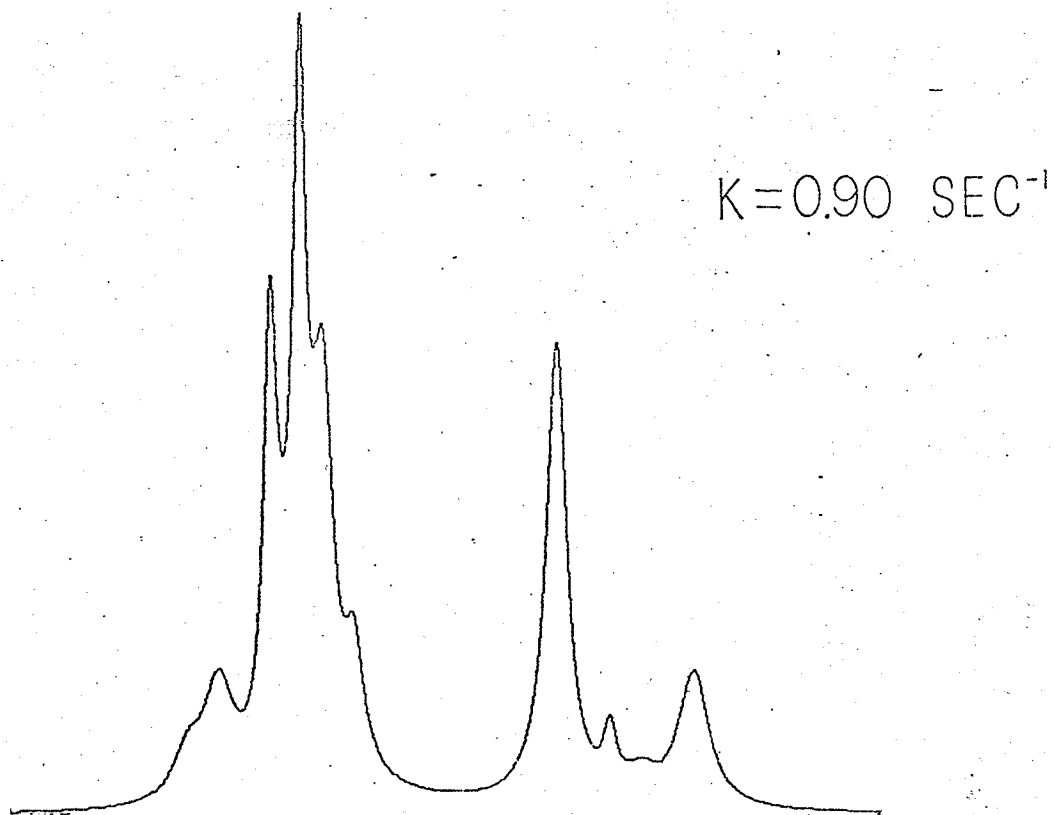
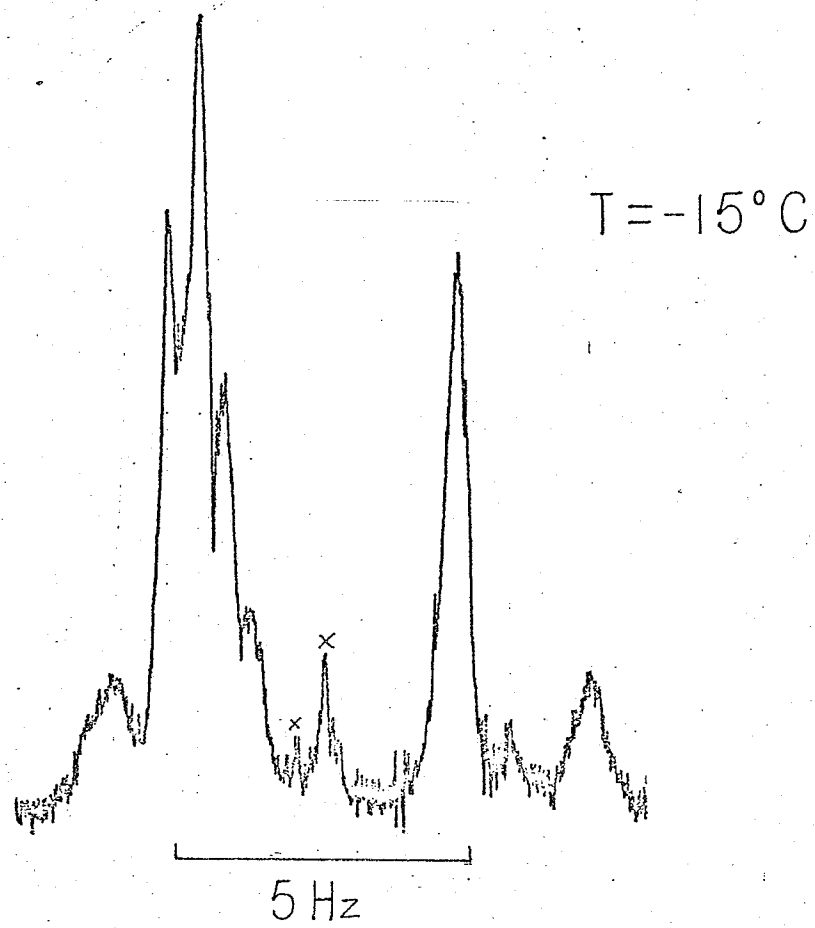


FIGURE 4

Experimental spectrum at 0°C and the  
corresponding calculated spectrum.

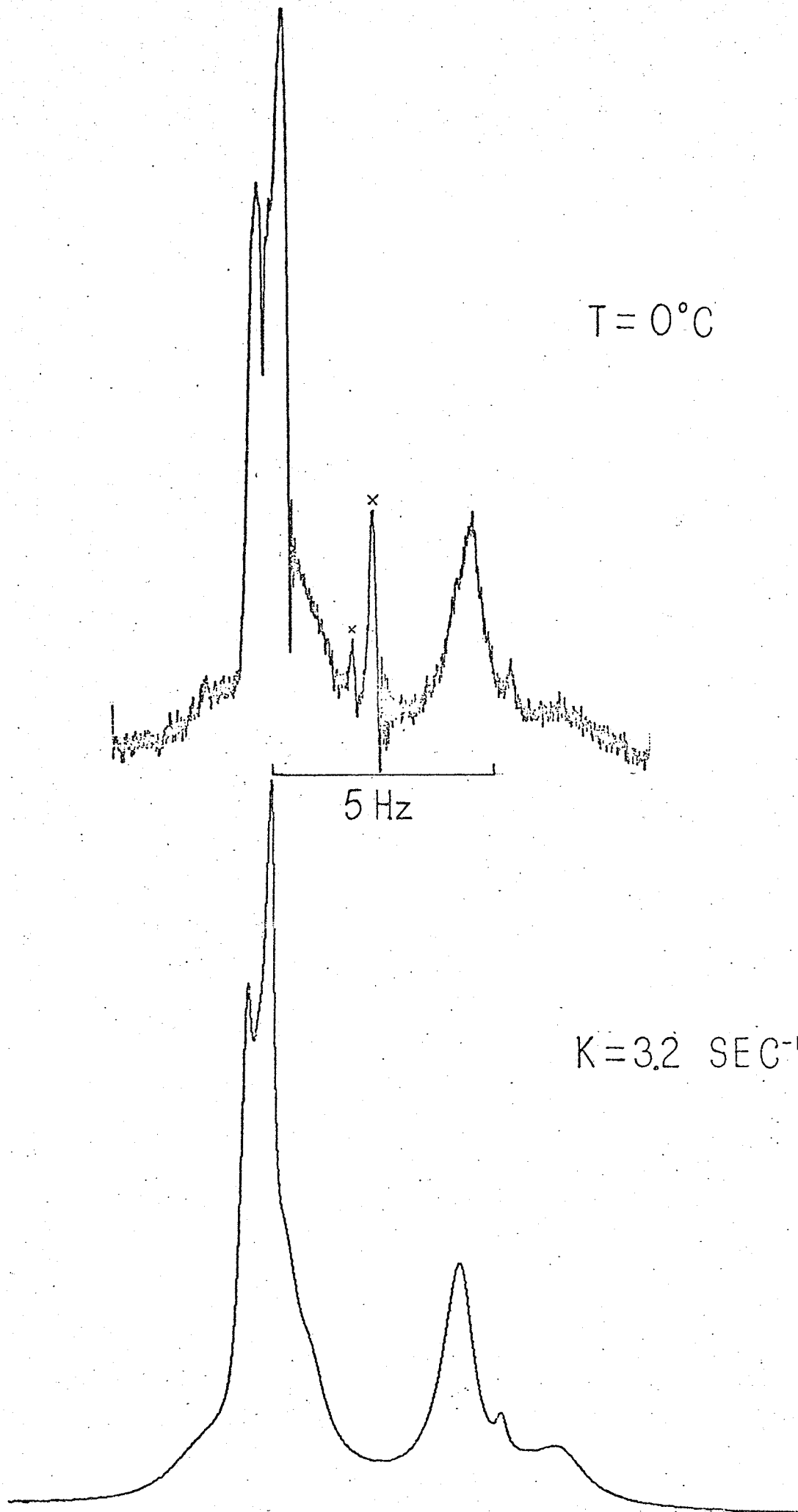


FIGURE 5

Experimental spectrum at 10°C and the  
corresponding calculated spectrum.

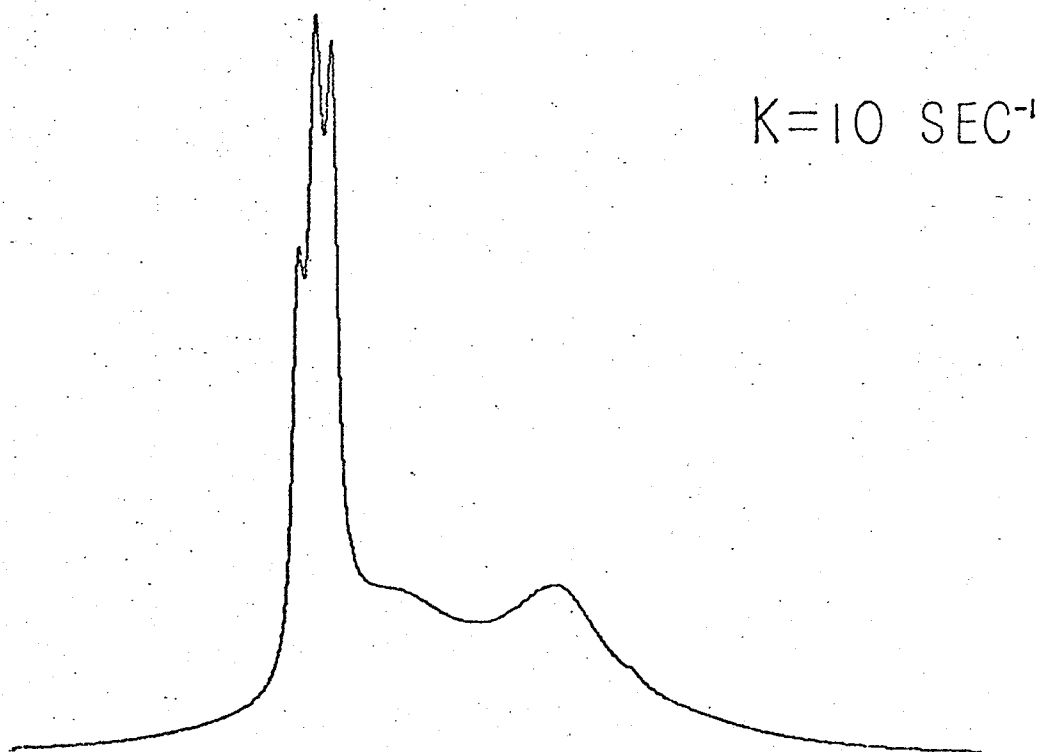
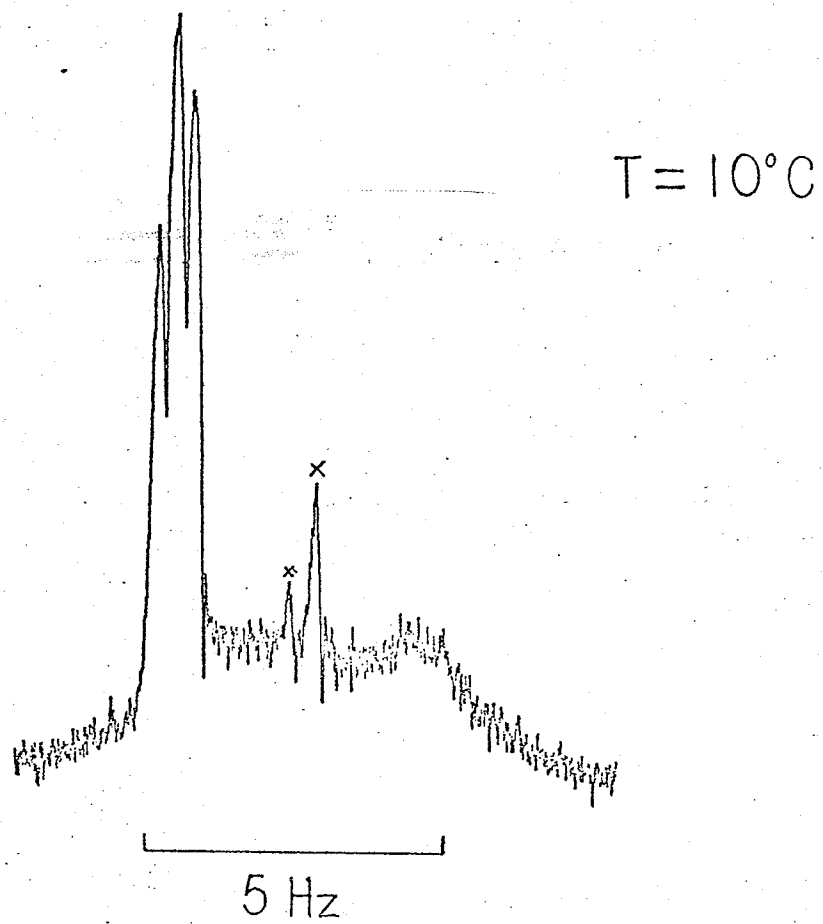


FIGURE 6

Experimental spectrum at 18°C and the  
corresponding calculated spectrum.

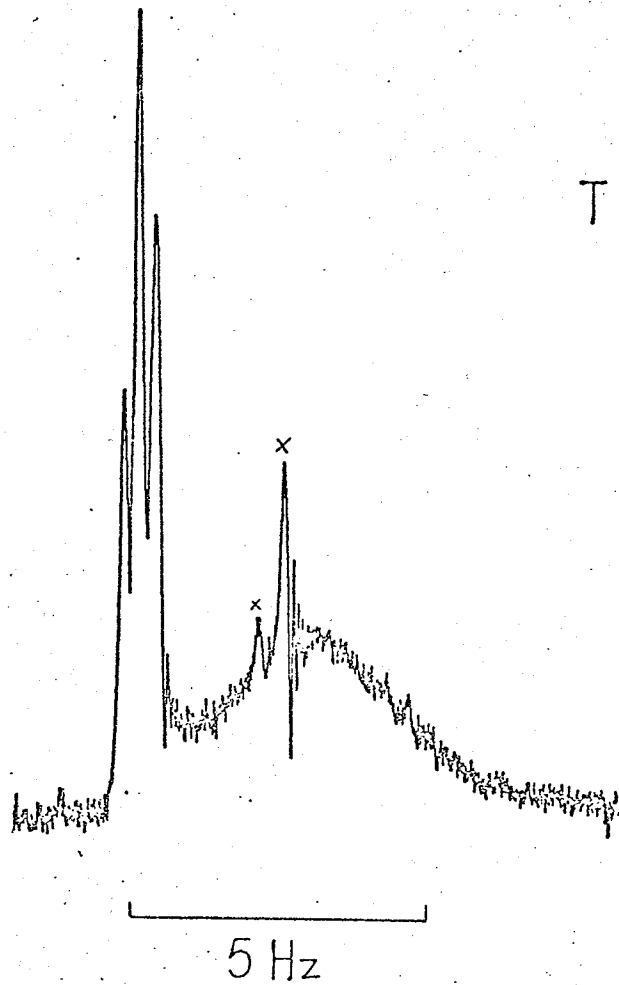
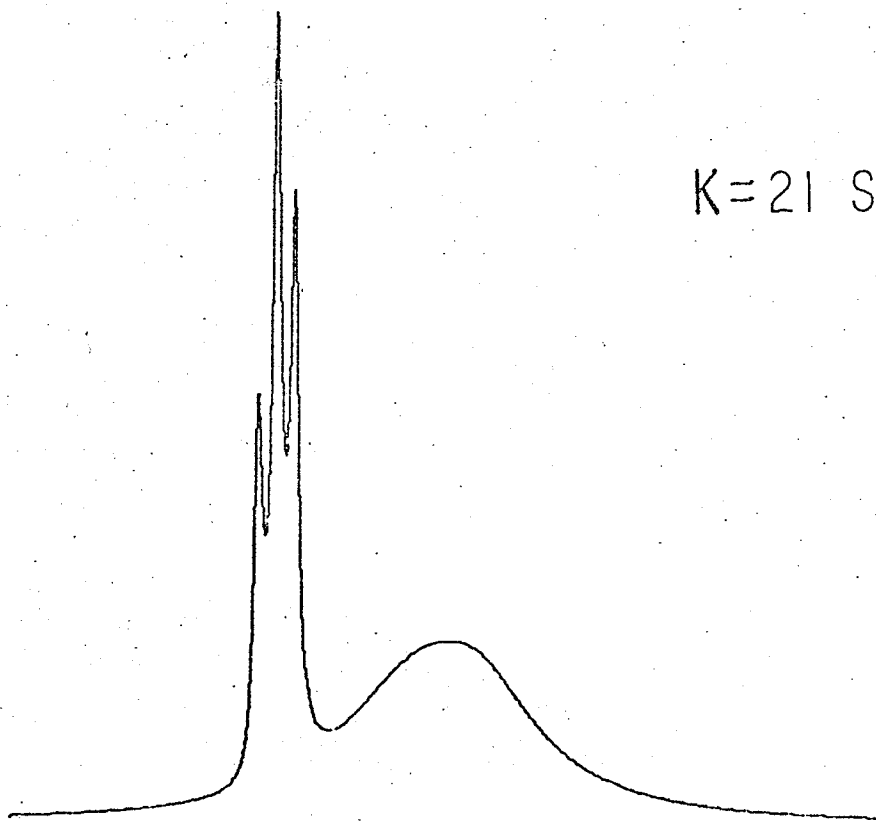
$T = 18^{\circ}\text{C}$  $K = 21 \text{ SEC}^{-1}$ 



FIGURE 7

Experimental spectrum at 30°C and the  
corresponding calculated spectrum.

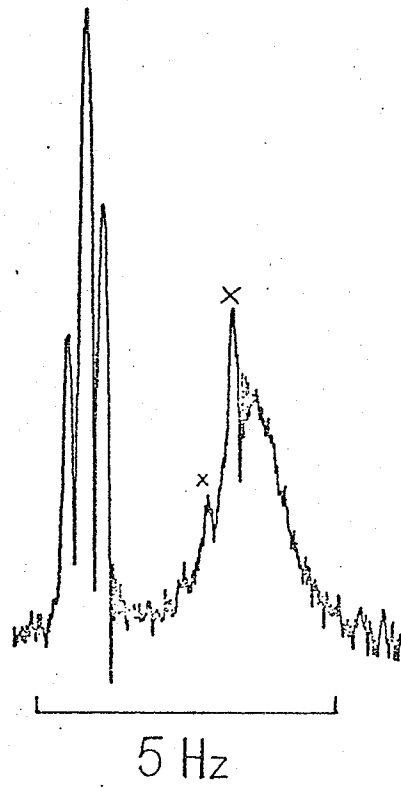
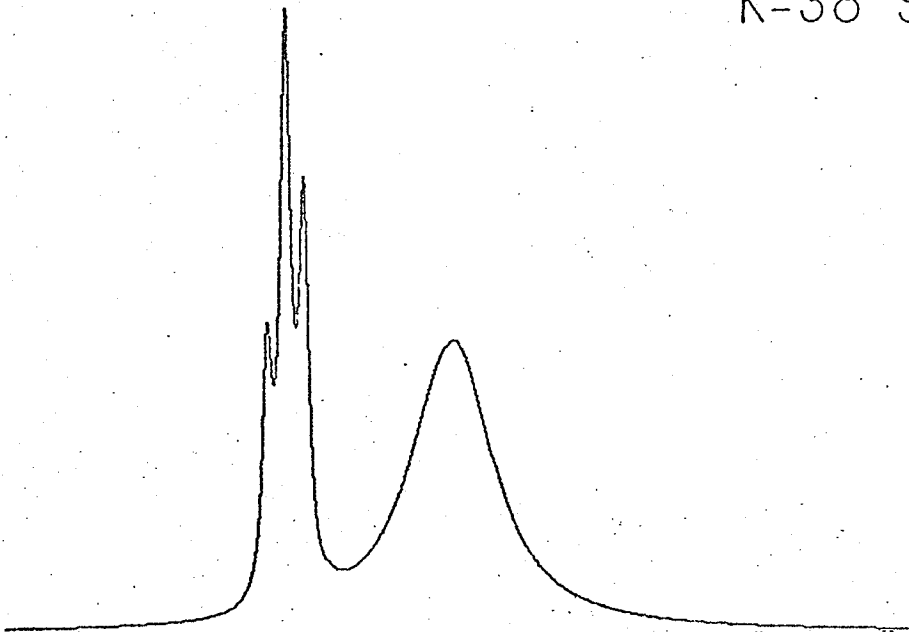
 $T = 30^\circ \text{C}$  $K = 38 \text{ SEC}^{-1}$ 

FIGURE 8

Experimental spectrum at 47°C and the  
corresponding calculated spectrum.

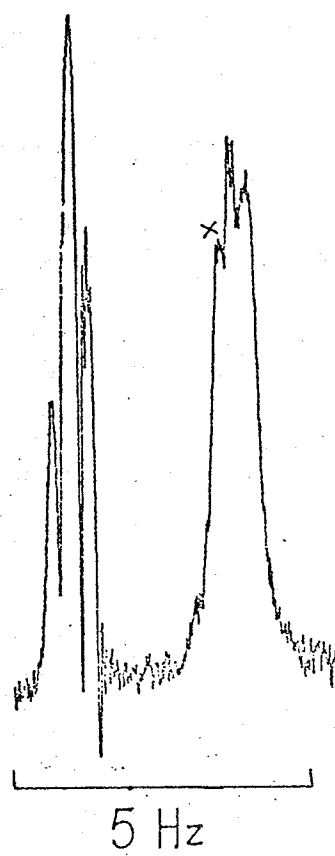
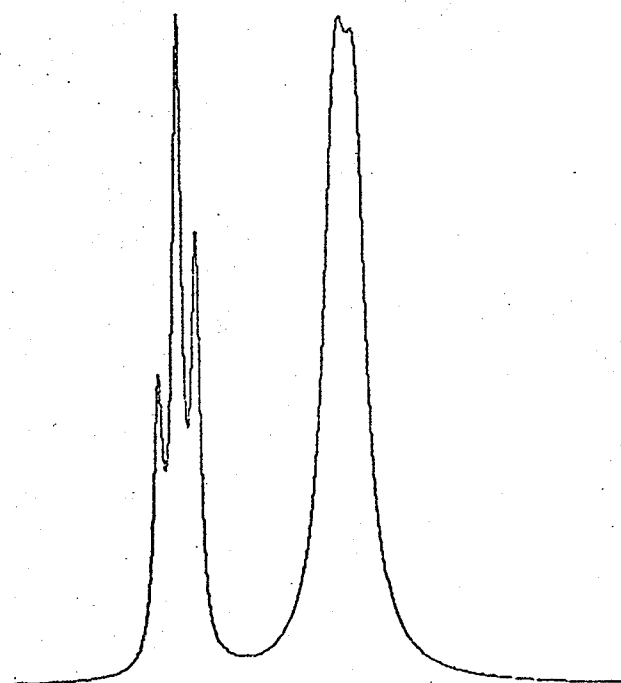
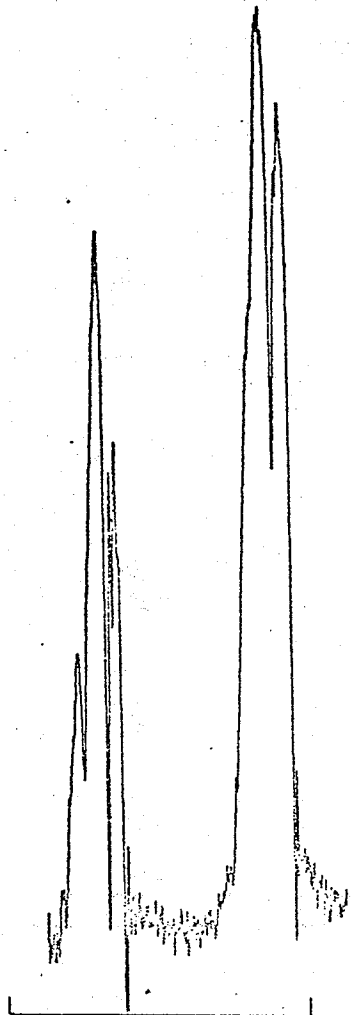
 $T = 47^{\circ}\text{C}$  $K = 160 \text{ SEC}^{-1}$

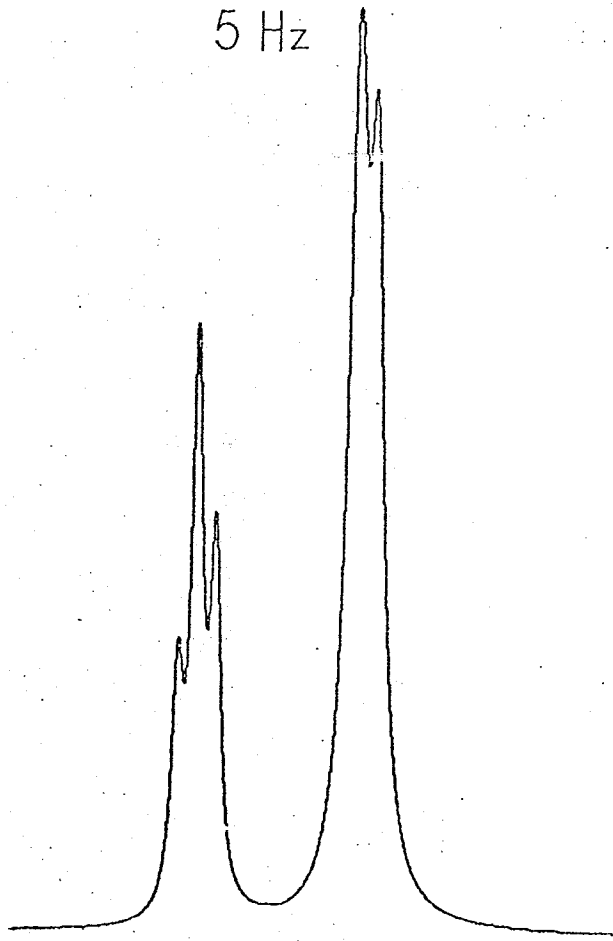
FIGURE 9

Experimental spectrum at 62°C and the  
corresponding calculated spectrum.



$T = 62^{\circ}\text{C}$

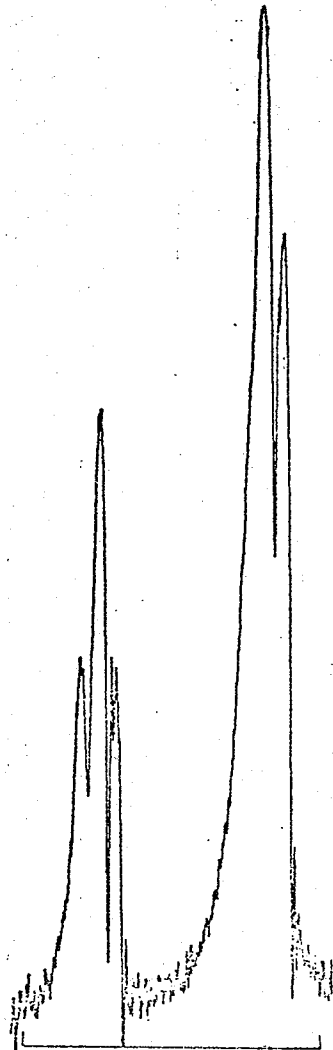
5 Hz



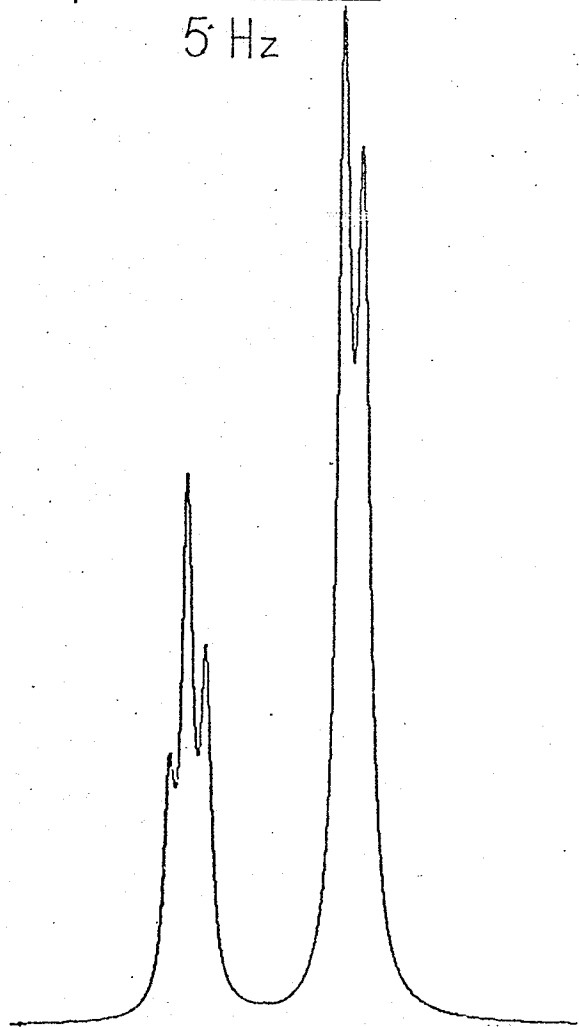
$K = 400 \text{ SEC}^{-1}$

FIGURE 10

Experimental spectrum at 73°C and the  
corresponding calculated spectrum.

$T = 73^{\circ}\text{C}$ 

5 Hz

 $K = 1000 \text{ SEC}^{-1}$ 



the effective relaxation time and is quite insensitive to the rate constant. For this reason, the line-shape fits at  $-34^{\circ}$ ,  $62^{\circ}$ , and  $73^{\circ}$  are not quite as reliable as the other six. The rate constants and their estimated errors are given along with the corresponding temperatures in Table 3.

TABLE 3

The rate constants and estimated errors for the hindered rotation in  $\alpha,\alpha,2,4,6$  - pentachlorotoluene at a series of temperatures.

Temperature ( $^{\circ}\text{C}$ )	Rate Constant ( $\text{sec}^{-1}$ )	Estimated Error ( $\text{sec}^{-1}$ )
-34	0.075	$\pm 0.025$
-15	0.90	$\pm 0.20$
0	3.2	$\pm 0.30$
10	10	$\pm 1$
18	21	$\pm 2$
30	38	$\pm 3$
47	160	$\pm 25$
62	400	$\pm 75$
73	1000	$\pm 200$

#### D. Calculation of the Thermodynamic Parameters

The energy of activation for the hindered rotation was calculated using the Arrhenius rate equation:

$$k = Ae^{-E_a/RT}, \quad 2.2$$

where  $k$  is the rate constant for the reaction,  $A$  is the "frequency factor",  $E_a$  is the energy of activation,  $R$  is the gas constant, and  $T$  is the absolute temperature. Equation 2.2 can be written in the form:

$$\log k = \log A - \frac{E_a}{2.303R} \left( \frac{1}{T} \right) \quad 2.3$$

A plot of  $\log k$  as a function of  $\frac{1}{T}$  yields  $\log A$  as the intercept and  $\frac{-E_a}{2.303R}$  as the slope. Analogously, the Eyring rate equation:

$$k = \frac{\kappa k_B T}{h} e^{-\frac{\Delta G^\ddagger}{RT}} = \frac{\kappa k_B T}{h} e^{-\frac{\Delta H^\ddagger}{RT}} e^{\frac{\Delta S^\ddagger}{R}}, \quad 2.4$$

can be written as:

$$\log \frac{k}{T} = \log \frac{\kappa k_B}{h} + \frac{\Delta S^\ddagger}{2.303R} - \frac{\Delta H^\ddagger}{2.303R} \left( \frac{1}{T} \right) \quad 2.5$$

A plot of  $\log \frac{k}{T}$  versus  $\frac{1}{T}$  yields a straight line with intercept  $\log \frac{\kappa k_B}{h} + \frac{\Delta S^\ddagger}{2.303R}$  and slope  $-\frac{\Delta H^\ddagger}{2.303R}$ , where  $\kappa$

is the transmission coefficient,  $k_B$  is the Boltzmann constant and  $h$  is Planck's constant. Therefore, one can obtain  $\Delta H^\ddagger$ , the enthalpy of activation, and  $\Delta S^\ddagger$ , the entropy of activation. The data required for calculating the thermodynamic parameters are listed in Table 4. In each case the best straight line was calculated by means of a least squares analysis using a computer program, called LSFIT3, written by Bruce Goodwin. The program calculates the slope and intercept, the corresponding standard deviations, and the correlation coefficient. Figures 11 to 14 show the plots obtained using LSFIT3. It is customary to report free energies of activation,  $\Delta G^\ddagger$ , for hindered rotations, although it is not a direct measure of the energy barrier. The free energy of activation for the hindered rotation of the molecule under consideration was calculated from the rate constant at 18°C using the Eyring rate equation, equation 2.4.

Thermodynamic activation parameters for the hindered rotation in  $\alpha,\alpha,2,4,6$ -pentachlorotoluene in toluene- $d_8$  and methylcyclohexane solutions were calculated by Fuhr (19). For purposes of comparison, Table 5 lists the results obtained for the three solutions. The last column in the table gives the activation parameters calculated by combining the rate data obtained for the individual solutions. As the table shows, the results agree within the quoted statistical errors.

TABLE 4

The data required for calculating the thermodynamic parameters.

<u>Temp. (°C)</u>	$\frac{1}{T} \times 10^3$	<u>k</u>	<u>log k</u>	$\frac{k}{T}$	<u>log <math>\frac{k}{T}</math></u>
-34	4.184	0.075	-1.1249	$3.0225 \times 10^{-4}$	-3.5197
-15	3.876	0.90	-0.0458	$3.483 \times 10^{-3}$	-2.4580
0	3.663	3.20	0.5051	$1.1712 \times 10^{-2}$	-1.9314
10	3.534	10.0	1.000	$3.53 \times 10^{-2}$	-1.4522
18	3.436	21.0	1.3222	$7.216 \times 10^{-2}$	-1.1417
30	3.300	38.0	1.5798	$1.254 \times 10^{-1}$	-0.9017
47	3.125	160.0	2.2041	$4.992 \times 10^{-1}$	-0.3017
62	2.985	400.0	2.6021	1.194	0.0770
73	2.890	1000.0	3.0000	2.890	0.4609

FIGURE 11

Arrhenius plot for the hindered rotation in  
 $\alpha,\alpha,2,4,6$ -pentachlorotoluene in 15 mole %  $\text{CS}_2$   
solution.

Parameters for this plot: slope:  $-3.11 \pm 0.06$

intercept:  $11.93 \pm 0.20$

correlation coefficient:  $-0.9989$

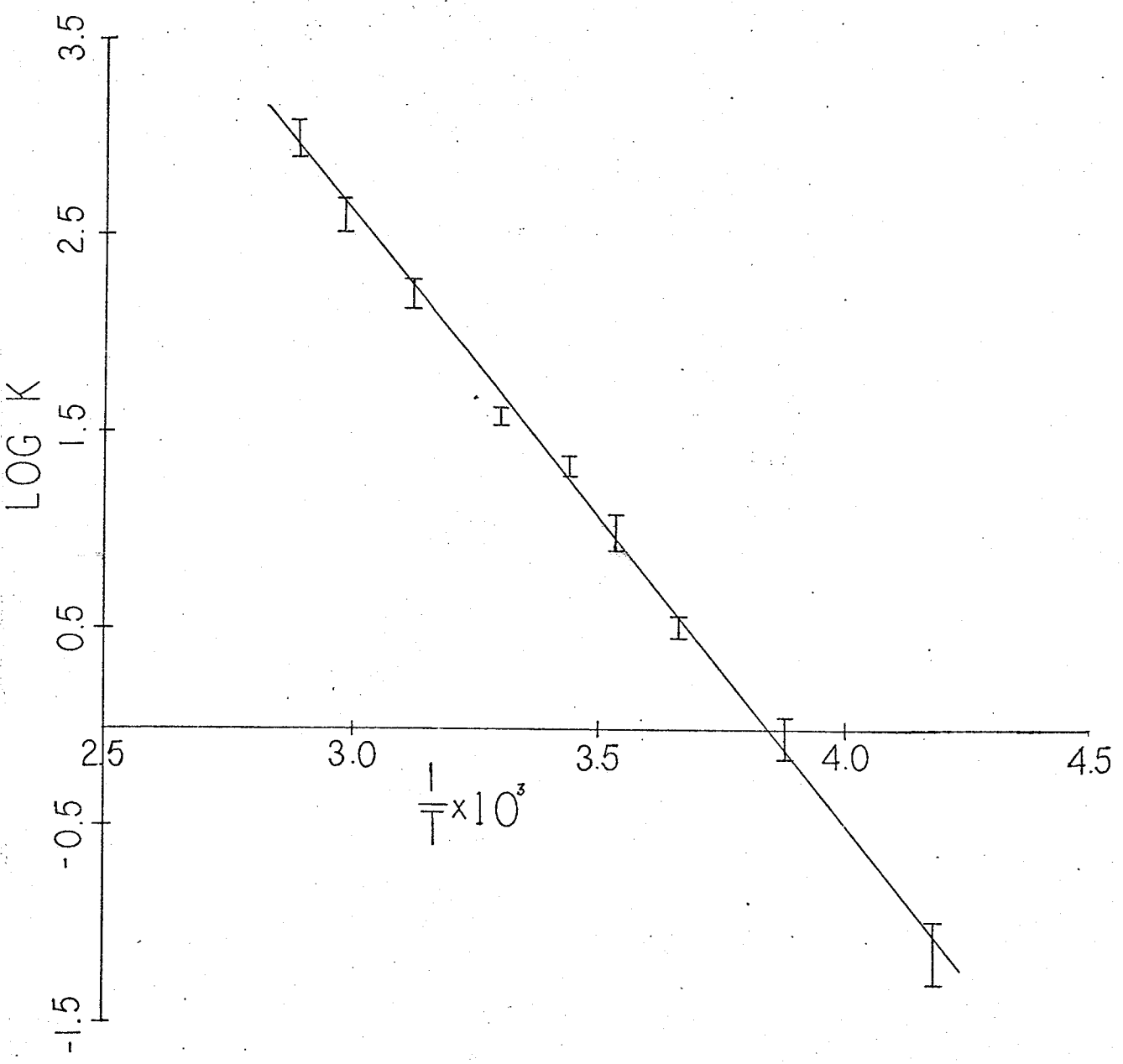


FIGURE 12

Eyring plot for the hindered rotation in  
 $\alpha,\alpha,2,4,6$ -pentachlorotoluene in 15 mole %  
 $\text{CS}_2$  solution.

Parameters for this plot: slope:  $-2.99 \pm 0.06$

intercept:  $9.06 \pm 0.20$

correlation coefficient:  $-0.9987$



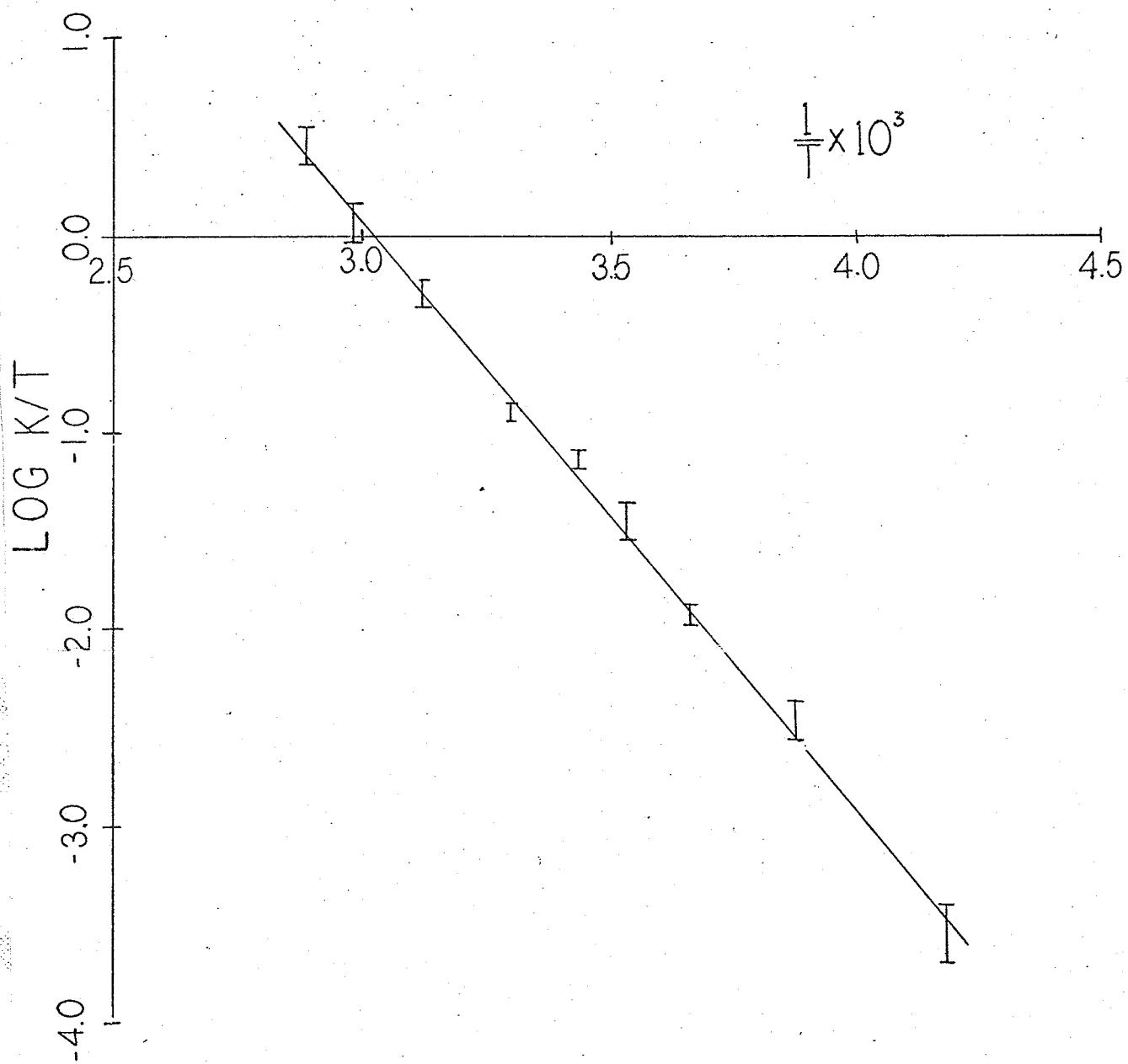


FIGURE 13

Arrhenius plot for the hindered rotation of  
 $\alpha,\alpha,2,4,6$ -pentachlorotoluene in the three solvents  
 $\text{CS}_2$ , toluene- $d_8$ , and methylcyclohexane.

○  $\text{CS}_2$  solution

△ toluene- $d_8$  solution

+ methylcyclohexane solution

Parameters for this plot: slope:  $-3.11 \pm 0.06$

intercept:  $11.95 \pm 0.20$

correlation coefficient:  $-0.9952$

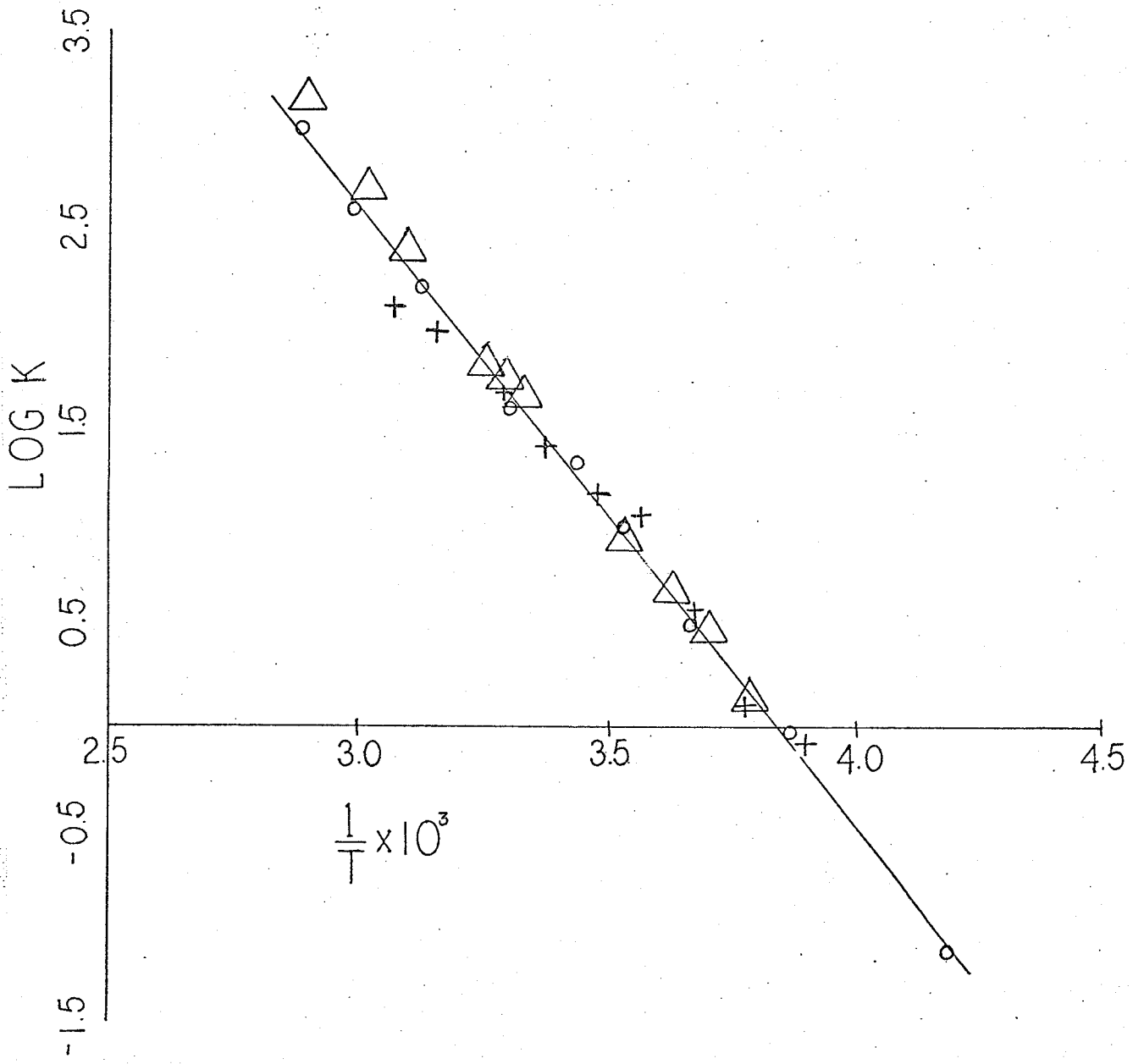


FIGURE 14

Eyring plot for the hindered rotation  $\alpha,\alpha,2,4,6$ -  
pentachlorotoluene in the three solvents  $\text{CS}_2$ ,  
toluene- $d_8$ , and methylcyclohexane.

○  $\text{CS}_2$  solution

△ toluene- $d_8$  solution

+ methylcyclohexane solution

Parameters for this plot: slope:  $-2.99 \pm 0.06$

intercept:  $9.06 \pm 0.21$

correlation coefficient: 0.9948

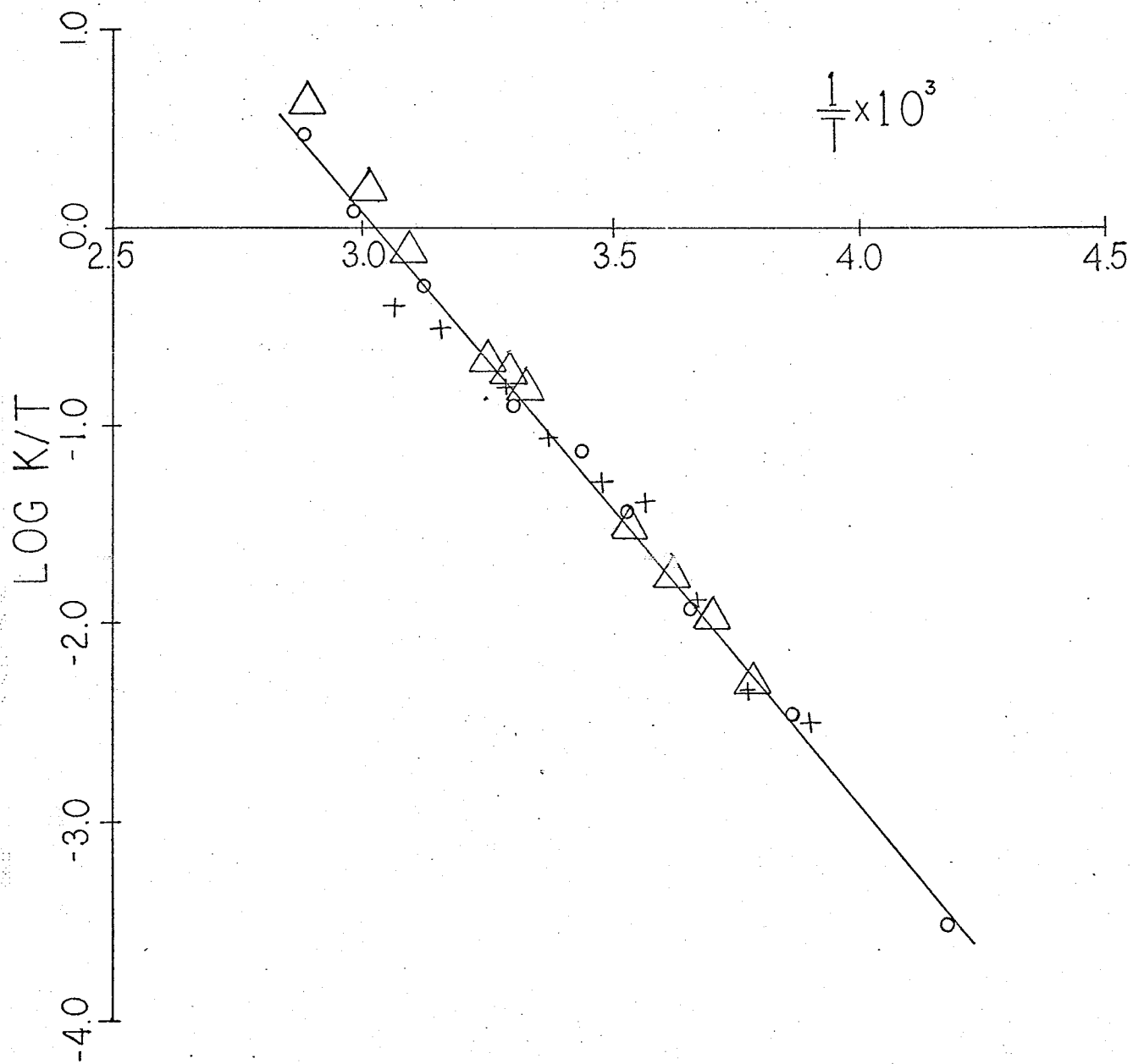


TABLE 5

Thermodynamic parameters<sup>†</sup> for the hindered rotation in  $\alpha,\alpha,2,4,6$  - pentachlorotoluene in three solutions.

Thermo- dynamic Parameter	Methyl- cyclohex- ane Solution	Toluene-d <sub>8</sub> Solution	CS <sub>2</sub> Solution	Three Solutions Combined
E <sub>a</sub>	14.3 ± 0.6	15.2 ± 0.2	14.22 ± 0.27	14.24 ± 0.27
log A	12.0 ± 0.5	12.7 ± 0.2	11.93 ± 0.20	11.95 ± 0.21
$\Delta H^\ddagger$	13.7 ± 0.6	14.6 ± 0.2	13.69 ± 0.27	13.68 ± 0.27
$\Delta S^\ddagger$	-4.4 ± 2.2	-1.1 ± 0.7	-4.38 ± 1.0	-4.37 ± 1.0
$\Delta G^\ddagger$	15.0 ± 0.2 (at 303.9°K)	14.9 ± 0.1 (at 303.5°K)	14.86 ± 0.10 (at 291°K)	---

<sup>†</sup> The quoted errors are standard deviations.

CHAPTER IV

DISCUSSION

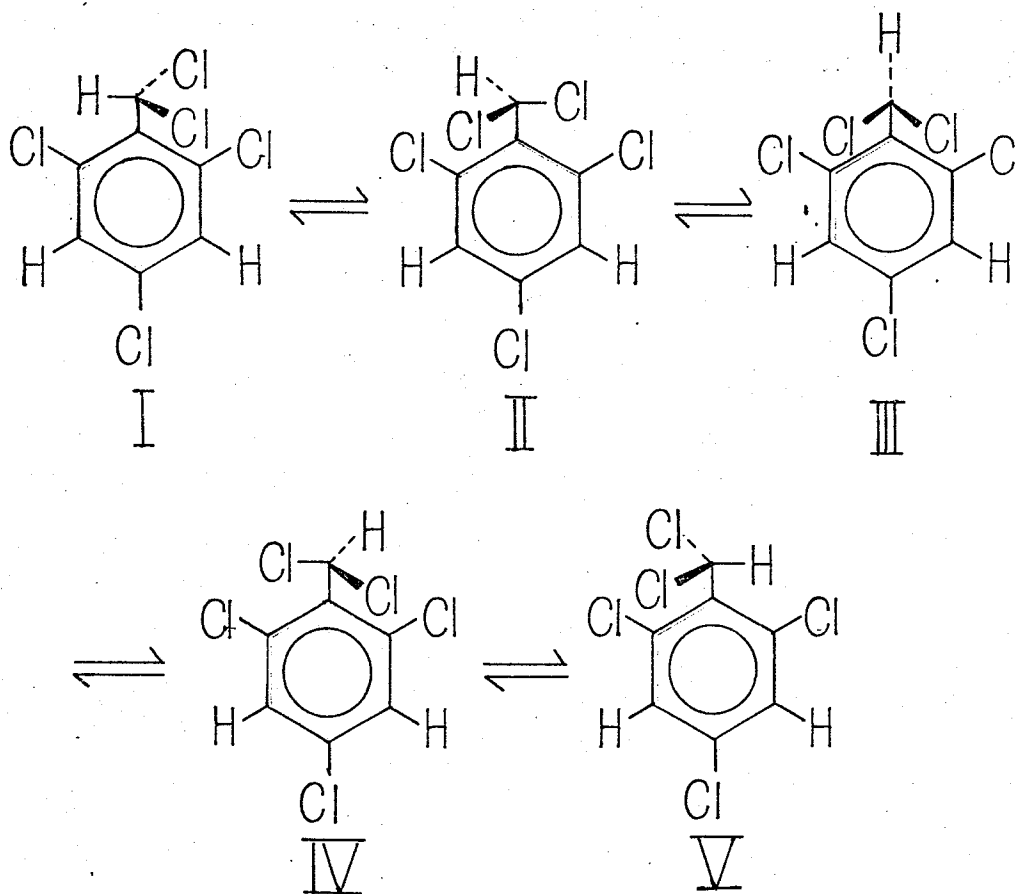
### A. The Energy Barrier to Rotation

It is known that rotations around single bonds in organic molecules are generally not free, but that certain factors hinder the rotation, giving rise to energy barriers of the order of several kilocalories per mole. Factors affecting the ease of rotation include steric crowding, electrostatic repulsion, resonance effects and hydrogen bonding. When one or more of these effects are present in a molecule, those conformations in which these are minimized will be favored, and hence not all possible conformations will be populated to a significant extent. Some factors which influence the magnitude of the energy barrier to rotation around single bonds have been discussed in detail with reference to polysubstituted ethanes (22,23) and propanes (24). Thompson, Newmark, and Sederholm (23) have shown that a correlation exists between the size of the barrier and the sum of the steric factors of the substituents in a series of halo-substituted ethanes. The steric factors used in their calculations are functions of the covalent radii of the substituents. Although several attempts have been made to explain quantitatively the experimental findings, no successful theory has yet been developed. A review of the work done on hindered internal rotations can be found in



references (1) and (25).

The energy barrier to rotation around the single bond in the molecule  $\alpha,\alpha,2,4,6$ -pentachlorotoluene (PCT), calculated in the previous chapter, will be discussed with reference to the five conformations:



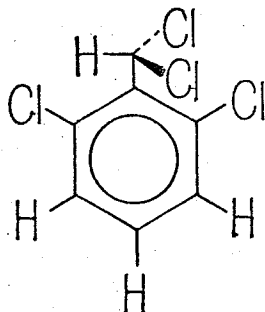
All the arrows represent  $60^\circ$  rotations except the ones between II and III, and III and IV which indicate  $30^\circ$  rotations. On the basis of the preceding discussion, conformers II and IV can be rejected at once as stable conformers because each of these has one of the side-

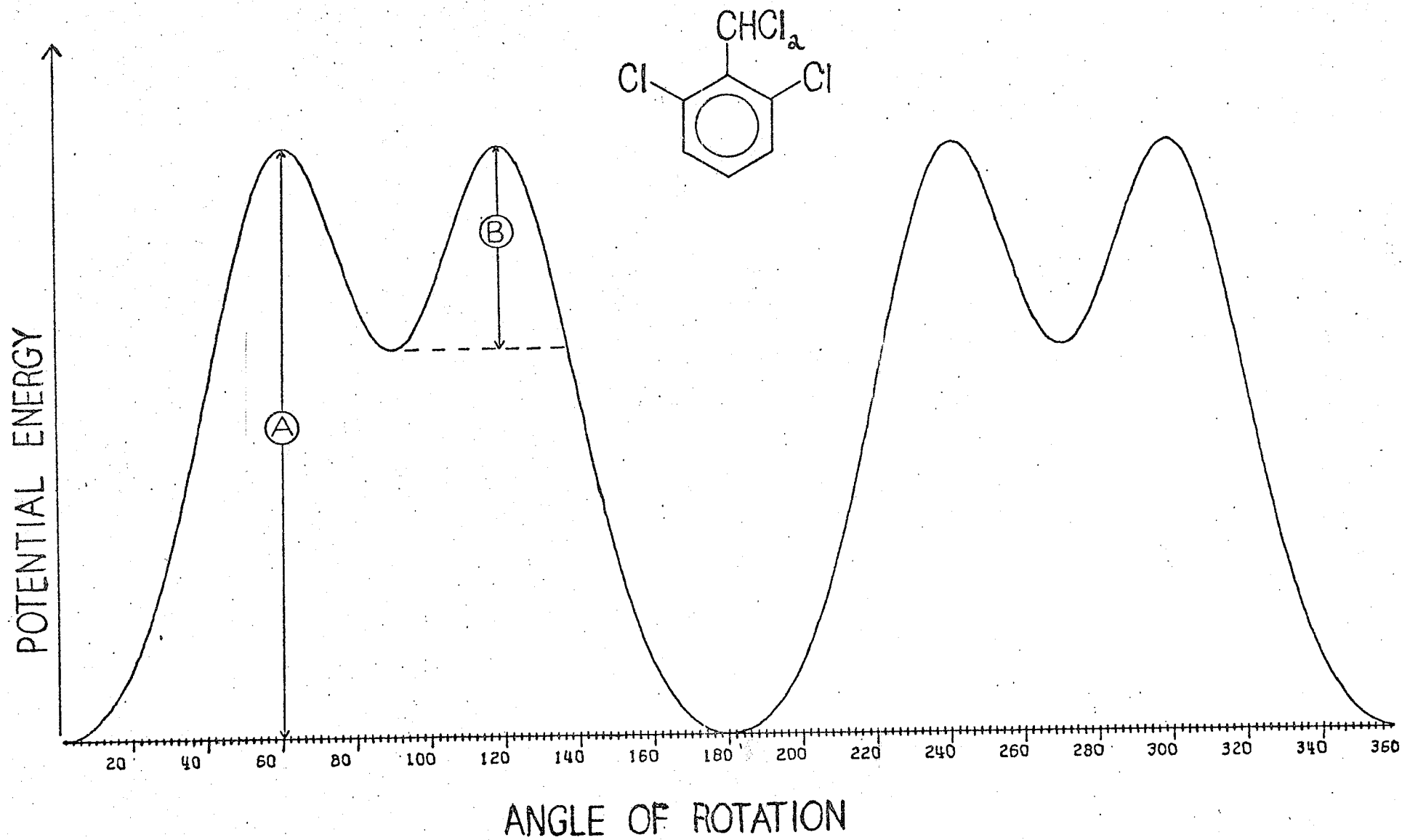
chain substituent chlorines in the plane of the ring and would thus be subject to maximum steric crowding from the adjacent ring chlorine atom. It is not immediately evident which of forms III or the pair I and V would be more energetically favorable. In conformer III both chlorines are  $30^\circ$  out of the plane of the ring, while in I and V they are both  $60^\circ$  out of the plane. If one considers only steric and electrostatic interactions, conformers I and V would appear to be most stable and hence most populated at low temperatures. The NMR spectrum of conformer III would be  $A_2B$  since the two ring protons are magnetically equivalent. The low temperature spectrum of the compound is in fact an ABC, indicating that the spectrum is that of the equivalent conformers I and V. That the sidechain proton most probably lies in the plane of the ring is also indicated by its stereospecific coupling to only one meta proton following the straightest zig-zag path (26), thus ruling out the presence of conformers II and IV at low temperatures. Potential energy calculations based on modified Buckingham and van der Waals functions carried out by Barber (25) verify these conclusions. The potential energy for the molecule  $\alpha,\alpha,2,6$ -tetrachlorotoluene as a function of the degree of rotation based on these calculations is shown in Figure 15.

FIGURE 15

The potential energy of  $\alpha,\alpha,2,6$ -tetrachlorotoluene as a function of degree of rotation of the dichloromethyl group, as calculated from a modified Buckingham potential energy function(25).

$0^\circ$  rotation corresponds to the conformation:





The absolute height of the barriers varies with the degree of bending of the ring C-Cl bonds, but the ratio of the barriers, A:B, is constant at 1:0.25. This potential energy diagram can be applied to PCT if the effect of the parachlorine atom on the barrier to rotation is neglected. A value of about 15 kilocalories mole<sup>-1</sup> for the barrier is obtained using the modified Buckingham function by allowing a 2° bending of the C-Cl bonds.

Because of the relatively high energy of conformer III it was assumed that if the molecule attained the energy required to overcome the initial barrier it would spend only a negligibly small amount of time in the potential well corresponding to conformer III and would be deactivated almost immediately to one of forms I or V. On this basis, and because of the symmetry of the potential energy diagram, the value of the transmission coefficient  $\kappa$  in the Eyring rate equation, defined as (22) "the rate of formation of deactivated product molecules produced by crossing the barrier under consideration in one direction divided by the rate of molecules crossing the barrier in that same direction", was given the value  $\frac{1}{2}$ . This procedure has been followed in previous work on this molecule (27) and also on  $\alpha,\alpha$ -dichloro-2,4,6-tribromotoluene (28). The value of

$14.2 \pm .3$  kilocalories mole<sup>-1</sup> found for the energy barrier to rotation of PCT in CS<sub>2</sub> agrees to within experimental error with that found for the same molecule in methylcyclohexane ( $14.3 \pm 0.6$ ) and toluene-d<sub>8</sub> ( $15.2 \pm 0.2$ ) solutions. The nature and extent of the effects of variations in the medium on energy barriers to rotation around single bonds is not known at present. One would expect, however, that increasing the dielectric constant of the medium would decrease the energy barrier for molecules in which electrostatic repulsion contributes appreciably to the barrier, since such forces are inversely proportional to the dielectric constant. Since the dielectric constants of CS<sub>2</sub>, toluene, and cyclohexane (that of methyl cyclohexane was not available) do not differ very much (2.641, 2.438, and 2.023 respectively), their effects on rotational barriers should be small.

The energy barrier to internal rotation in the molecule  $\alpha,\alpha$ -dichloro-2,4,6-tribromotoluene was calculated by a total lineshape method (28) following the theory described by Goodwin (15). The reported value is 16.38 kilocalories mole<sup>-1</sup> which is slightly higher than that found for PCT. This result may be attributed to the increased steric crowding in the transition state of the molecule due to the greater bulk of the bromine atoms in the ortho positions.

## B. Errors

It has by now come to the attention of most authors in the field that rate determinations by NMR methods are susceptible to severe systematic errors. An extensive analysis of the nature and magnitude of systematic errors incurred in studying chemical exchange rates by steady state and pulsed NMR techniques has been done by Allerhand, Gutowsky, Jonas, and Meinzer (29).

Systematic errors in calculating rate constants arise from three sources: the mathematical model, the experimental procedure, and the method of fitting theoretical to experimental spectra. Since the advent of exact quantum mechanical lineshape theories, the practice of using approximate models in cases where they do not apply has decreased. Several computer programs incorporating the complete lineshape theories of Alexander (30, 31, 32) and Johnson (33) are now available. The most versatile lineshape program available at present is DNMR (18), the one used in this work. Because the mathematical model on which it is based is free from approximations of questionable validity, one can be confident that its use will not introduce systematic errors into the calculation of rate constants. There is one assumption, however, which has to be made in order to make the solution of the equation of motion of the density matrix

possible. One has to assume a steady state condition, although this cannot be met in an actual experiment. It can be very closely approximated by recording the spectra at very slow sweep rates, although this introduces spectral distortions due to saturation effects. These distortions can be minimized by using a radio-frequency field of small amplitude. In the present work the  $H_1$  field never exceeded 0.02mgauss. The effect of sweep rates and radiofrequency field amplitudes on lineshapes was examined by Grunwald, Loewenstein, and Meiboom (34), who found that a sixfold variation in sweep rate and a hundred fold variation in  $H_1$  left the values of the ratio of maximum to central minimum intensity of a recorded spectrum essentially constant. Excessive filtering must also be avoided if one is to prevent distortion of spectral lines. Other factors which may influence the lineshapes are field inhomogeneities and temperature fluctuations. The important thing to remember about the various systematic errors introduced by the experimental method is that they cannot be completely avoided and their complexity makes it impossible for them to be quantitatively estimated. It is therefore of paramount importance to minimize them as much as possible by recording the spectra under optimum conditions.



The third source of systematic errors in NMR rate determinations is the fitting of the spectra. It is not always possible to obtain exactly the static parameters required for computing the theoretical line-shapes. Chemical shifts and coupling constants can be determined only at very slow exchange rates and one must use extrapolation techniques to obtain them in the coalescence region. The temperature dependence of chemical shifts in solvents which give rise to large solvent induced shifts can often be assumed to be a linear one. The usual procedure is to analyse several low temperature spectra to obtain the temperature dependence of the chemical shifts and then extrapolate to higher temperatures. However, the temperature range in which the spectra can be analysed is quite limited by the solubility and exchange broadening. Obtaining the correct  $T_2$  value is also a difficult problem. Since the effective  $T_2$  is largely dependent on instrumental conditions, the best procedure is to measure it at each temperature studied. If one of the peaks remains sharp throughout the exchange process, it can be used to monitor the homogeneity of the field, and its half-height linewidth can be used to calculate the effective  $T_2$  as in equation 2.1. If this is not the case, then the resonance line due to a compound closely related to the

one being studied may be used. In the present work, the  $T_2$  at the six lower temperatures was obtained from the half-height linewidth of the impurity peak due to  $\alpha, \alpha, \alpha, 2, 4, 6$ -hexachlorotoluene which always gave a sharp resonance line. At the three higher temperatures, however, this peak became obscured by the doublet due to the two ring protons of PCT, so that the  $T_2$  had to be estimated from the linewidth of the methine proton resonance. The error introduced into the rate constant by an error in  $T_2$  is significant only toward the two extremes of slow and fast exchange, where the lineshape is decreasingly sensitive to the rate of exchange. Therefore, if a reasonably large number of spectra are fitted in the intermediate region, the resulting thermodynamic parameters may be quite reliable in spite of errors in  $T_2$ , if spectral distortions in this region are kept at a minimum.

It was found that the effect of  $T_2$  on the lineshapes of computed spectra at high exchange rates was most predominant in the width and the amount of splitting of the lines, and did not greatly affect their relative intensities. On the other hand, varying the rate constant in this range produced no significant change in the linewidths but did alter their relative heights. Therefore, when the spectra at the higher temperatures were fitted, the relative heights of the

absorption lines were given greater consideration in determining the rate constants. From these considerations it appears that the fitting of lineshapes by a single characteristic parameter such as the half-height linewidth or the peak to peak separation can lead to systematic errors. A matching of the overall lineshape is more desirable. Furthermore, a more complicated spectrum will have more variations in the lineshape as a function of the exchange rate and hence more reliable lineshape fits can be obtained. In this work, the lineshapes were fitted by superimposing the theoretical spectra on the experimental ones and the best fit was obtained visually. The estimated errors in the fits are represented by the error bars in Figures 11 and 12. The ideal method for fitting theoretical to experimental spectra is that used by Jonas, Allerhand, and Gutowsky (35) in determining thermodynamic parameters for the chair-chair isomerization of 1,1-difluorocyclohexane. The experimental spectrum is entered in the computer as a set of digitized absorption intensities and compared to theoretical spectra with a series of rate constants and the best least squares fit is obtained.

The effect of systematic errors in the rate constants on the calculated thermodynamic parameters was examined by Allerhand, Chen, and Gutowsky (36). They collected

the available thermodynamic data on cyclohexane and  $d_{11}$ -cyclohexane and on comparison found large deviations in  $\Delta H^\ddagger$  and  $\Delta S^\ddagger$  but found good agreement in  $\Delta G^\ddagger$  values. They developed a set of equations which show that systematic errors affect  $\Delta H^\ddagger$ , dominate  $\Delta S^\ddagger$ , but do not affect  $\Delta G^\ddagger$ . The maximum errors in the thermodynamic parameters for the hindered rotation in PCT were obtained by taking into account the uncertainty in the rate constants represented by the error bars in Figures 11 and 12. Two straight lines, passing through the extrema of the error bars and pivoting at the coalescence temperature, may be drawn through each set of points, yielding the maximum and minimum values for the slopes and intercepts of the Arrhenius and Eyring plots. These values are then used to calculate the absolute confidence limits for the thermodynamic parameters. Table 6 lists the results of these calculations. It was found that the errors obtained in this way are approximately three times as large as the standard deviations, indicating the presence of systematic errors.

TABLE 6

Maximum and minimum values\* for the thermodynamic parameters.

Thermodynamic Parameter	Maximum Value	Minimum Value
$E_a$	15.17 kcal/mole.	13.36 kcal/mole.
log A	12.62	11.29
$\Delta H^\ddagger$	14.64 kcal/mole.	12.78 kcal/mole.
$\Delta S^\ddagger$	-1.2 e.u.	-7.48 e.u.

\* obtained as described in the text

CHAPTER V

CONCLUSION

The complete lineshape theory of exchange broadened NMR spectra devised by Binsch has been described. The computer program DNMR based on this theory was used to calculate theoretical spectra for a series of rate constants of the exchange due to the hindered internal rotation in the molecule  $\alpha,\alpha,2,4,6$ -pentachlorotoluene. It was found that because of the great variation of the lineshape as a function of the exchange rate, it was a relatively simple matter to fit experimental and calculated spectra. However, in spite of the absence of approximations in the theory, the method of lineshape fitting for the determination of rate constants is still vulnerable to certain systematic errors which are difficult to avoid. The main sources of systematic errors are the approximate methods used to determine the static parameters and the unavoidable imperfections in the experimental spectra.

The activation parameters obtained agree with those obtained using an independent lineshape theory and computer program (19), suggesting that fitting errors are not large. The experimental spectra were of different types (ABC and ABX) in the two procedures, again suggesting that the measured lineshapes did not suffer unduly from distortions.

CHAPTER VI

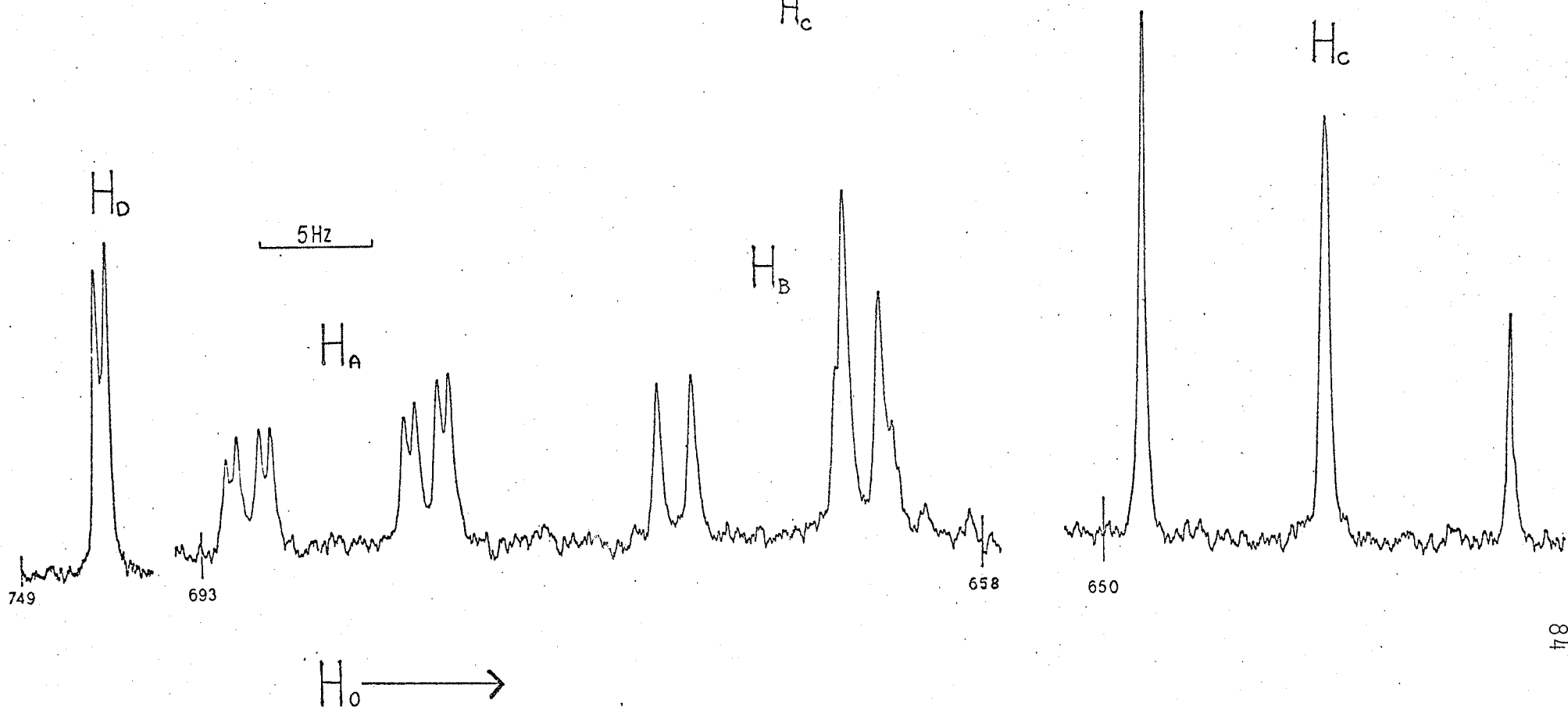
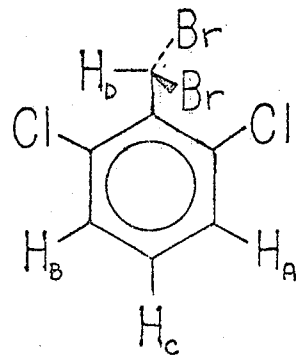
SUGGESTIONS FOR FUTURE RESEARCH



It has been pointed out that the theory outlined in this thesis is readily applicable to complicated spin systems. In fact, more reliable results can be obtained if the spectrum has more than one coalescence region. It would therefore be an interesting problem to study the hindered rotation in the molecule  $\alpha,\alpha$ -dibromo-2,6-dichlorotoluene whose NMR spectrum at room temperature, where the exchange rate is very slow, is an ABCD. The spectrum is shown in Figure 16. It consists, to a first order approximation, of a doublet, an octet, a quartet and a triplet. The doublet is assigned to  $H_D$ , the methine proton, the octet to  $H_A$  because it is coupled to each of the other protons, the quartet to  $H_B$ , and the triplet to  $H_C$ . A quartet is actually expected for  $H_C$ , but because the coupling constants  $J_{AC}$  and  $J_{BC}$  are very nearly equal, the two middle lines overlap giving a triplet. It is expected that at higher temperatures the lines due to  $H_A$  and  $H_B$  will broaden and coalesce, and finally appear as a quartet at very high temperatures. As in  $\alpha,\alpha,2,4,6$ -pentachlorotoluene, the methine proton resonance will probably stay sharp at all temperatures but change to a triplet at high exchange rates when the apparent chemical shifts of  $H_A$  and  $H_B$  become equivalent. The  $H_C$  resonance at high exchange rates is expected to be a triplet although the relative intensities of the

FIGURE 16

The room temperature proton magnetic resonance spectrum of  $\alpha,\alpha$ -dibromo-2,6-dichlorotoluene at 60 MHz.



lines may change. It is difficult to predict exactly how the lines due to  $H_C$  will change with temperature because the spectrum is far from first order. The molecule  $\alpha,\alpha,2,6$ -tetrachlorotoluene gives an NMR spectrum very similar to that of  $\alpha,\alpha$ -dibromo-2,6-dichlorotoluene. The hindered rotation of the dichloromethyl group will produce the same changes in lineshape as a function of temperature as will occur in the spectrum of the latter compound. However, coalescence of the lines occurs at a lower temperature, which may be an indication that the energy barrier to rotation is lower in this compound, although this does not necessarily follow. The difference may be accounted for in terms of the magnitude of the frequency factor which is related to the entropy of activation. In any case, this question could be resolved by doing a complete lineshape analysis of both compounds and comparing the results. In addition, such a comparison may also shed some light on the problem of describing the factors affecting internal rotations in molecules.

BIBLIOGRAPHY

1. G.Binsch, Topics in Stereochemistry, Edited by E.L.Eliel and N.L.Allinger, Interscience Publishers 1968 Volume 3.
2. C.S.Johnson, Jr., Advances in Magnetic Resonance, Edited by J.S.Waugh, Academic Press 1965 Volume 1.
3. H.S.Gutowsky, D.McCall, and C.P.Slichter: J.Chem. Phys. 21, 729 (1953)
4. H.S.Gutowsky and A.Saika: J.Chem.Phys. 21, 1688 (1953)
5. H.S.Gutowsky and R.Holm: J.Chem.Phys. 25, 1228 (1956)
6. U.Fano: Rev.Mod.Phys. 29, 74 (1957)
7. J.Kaplan: J.Chem.Phys. 28, 278 (1958)
8. J.Kaplan: J.Chem.Phys. 29, 462 (1958)
9. S.Alexander: J.Chem.Phys. 37, 967 (1962)
10. S.Alexander: J.Chem.Phys. 37, 974 (1962)
11. C.S.Johnson, Jr.: J.Chem.Phys. 41, 3277 (1964)
12. C.S.Johnson, Jr.: J.Mag.Res. 1, 98 (1969)
13. U.Fano, Lectures on the Many Body Problem, Edited by E.R.Caianiello., Academic Press, 1964 Volume 2.
14. G.Binsch, J.Am.Chem.Soc. 91, 1304 (1969)
15. B.Goodwin, M.Sc. Thesis, University of Manitoba, 1969
16. G.Binsch: J.Mol.Phys. 15, 469 (1968)
17. G.M.Whitesides, Ph.D. Thesis, California Institute of Technology, 1964
18. G.Binsch and D.A.Kleier, University of Notre Dame, Indiana
19. B.Fuhr, M.Sc. Thesis, University of Manitoba, 1969.

20. C.N.Banwell and N.Sheppard, Discussions Faraday Soc. 34, 115 (1962)
21. K.Dahlqvist and S.Forsén, J.Phys.Chem. 73, 4124 (1969)
22. R.Newmark and C.Sederholm: J.Chem.Phys. 43, 602 (1965)
23. D.S.Thompson, R.Newmark, and C.Sederholm: J.Chem. Phys. 37, 411 (1962)
24. A.B.Dempster, K.Price, and N.Sheppard: Spectrochimica Acta, Vol. 25A, 1381 (1969)
25. B.Barber, M.Sc. Thesis, University of Manitoba, 1970
26. T.Schaefer, R.Schwenk, C.J.Macdonald, and W.F.Reynolds, Can.J.Chem. 46, 2187 (1968)
27. B.Fuhr, B.W.Goodwin, H.M.Hutton and T.Schaefer, Can.J.Chem. 48, 1558 (1970)
28. J.Peeling, T.Schaefer, and C.M.Wong, Can.J.Chem. in press.
29. A. Allerhand, H.S.Gutowsky, J.Jonas, and R.A.Meinzer, J.Am.Chem.Soc. 88, 3185 (1966)
30. J.Heidberg, J.A.Weil, G.A.Janusonis, and J.K.Anderson, J.Chem.Phys. 41, 1033 (1964)
31. J.M.Lehn, F.G.Riddell, B.J.Prince, and I.O.Sutherland, J.Chem.Soc.(B), 387 (1967)
32. R.J.Kurland, M.B.Rubin, and W.B.Wise, J.Chem.Phys. 40, 2426 (1964)
33. C.S.Johnson, Jr., J.Mag.Res. 1, 98 (1969)
34. E.Grunwald, A.Loewenstein, and S.Meiboom, J.Chem.Phys. 27, 630 (1957)
35. J.Jonas, A.Allerhand, and H.S.Gutowsky, J.Chem.Phys. 42, 3396 (1965)
36. A.Allerhand, F.Chen, and H.S.Gutowsky, J.Chem.Phys. 42, 3040 (1965)
37. S.Castellano and A.A.Bothner-By, J.Chem.Phys. 41, 3863 (1964); LAOCN3, Mellon Institute, Pittsburgh, Pa., 1966

APPENDIX I



DERIVATION OF THE VECTORS  $U^{(j)}$  WHICH CONSTITUTE  
THE BASIS OF A SIXTEEN DIMENSIONAL VECTOR SPACE.

Consider four spin operators defined<sup>1</sup> as:

$$\begin{aligned} E|\alpha\rangle &= |\alpha\rangle, & E|\beta\rangle &= |\beta\rangle \\ I_x|\alpha\rangle &= |\beta\rangle, & I_x|\beta\rangle &= |\alpha\rangle \\ I_y|\alpha\rangle &= i|\beta\rangle, & I_y|\beta\rangle &= -i|\alpha\rangle \\ I_z|\alpha\rangle &= |\alpha\rangle, & I_z|\beta\rangle &= -|\beta\rangle \end{aligned} \quad 7.1$$

The two spin functions  $|\alpha\rangle$  and  $|\beta\rangle$  can be represented  
in matrix notation as:

$$|\alpha\rangle = \begin{bmatrix} 1 \\ 0 \end{bmatrix} \quad \text{and} \quad |\beta\rangle = \begin{bmatrix} 0 \\ 1 \end{bmatrix} \quad 7.2$$

Using the definitions given by equations 7.1 and 7.2 the  
four operators can be represented as:

$$E = \begin{bmatrix} 1 & 0 \\ 0 & 1 \end{bmatrix}; \quad I_x = \begin{bmatrix} 0 & 1 \\ 1 & 0 \end{bmatrix}; \quad I_y = \begin{bmatrix} 0 & -i \\ i & 0 \end{bmatrix}; \quad I_z = \begin{bmatrix} 1 & 0 \\ 0 & -1 \end{bmatrix} \quad 7.3$$

For example:  $I_x|\alpha\rangle = \begin{bmatrix} 0 & 1 \\ 1 & 0 \end{bmatrix} \begin{bmatrix} 1 \\ 0 \end{bmatrix} = \begin{bmatrix} 0 \\ 1 \end{bmatrix} = |\beta\rangle$

Consider now a two-spin system with the four possible  
spin states:  $|\alpha\alpha\rangle, |\alpha\beta\rangle, |\beta\alpha\rangle, |\beta\beta\rangle$ . Their matrix repre-  
sentations are obtained by taking the direct product of  
the matrices representing the spin state of each individu-  
al particle. Hence:

---

1. The constant  $\frac{1}{2}$  was omitted for convenience. This has  
no effect on the result.

$$|\alpha\alpha\rangle = \begin{bmatrix} 1 \\ 0 \end{bmatrix} \otimes \begin{bmatrix} 1 \\ 0 \end{bmatrix}; \quad |\alpha\beta\rangle = \begin{bmatrix} 1 \\ 0 \end{bmatrix} \otimes \begin{bmatrix} 0 \\ 1 \end{bmatrix}; \quad |\beta\alpha\rangle = \begin{bmatrix} 0 \\ 1 \end{bmatrix} \otimes \begin{bmatrix} 1 \\ 0 \end{bmatrix}; \quad |\beta\beta\rangle = \begin{bmatrix} 0 \\ 1 \end{bmatrix} \otimes \begin{bmatrix} 0 \\ 1 \end{bmatrix}$$

7.4

The direct product of two matrices A and B is defined as:

$$(A \otimes B)_{ik,jl} = A_{ij} B_{kl} \quad 7.5$$

Therefore the spin states of a two spin system are represented as:

$$|\alpha\alpha\rangle = \begin{bmatrix} 1 \\ 0 \\ 0 \\ 0 \end{bmatrix}; \quad |\alpha\beta\rangle = \begin{bmatrix} 0 \\ 1 \\ 0 \\ 0 \end{bmatrix}; \quad |\beta\alpha\rangle = \begin{bmatrix} 0 \\ 0 \\ 1 \\ 0 \end{bmatrix}; \quad |\beta\beta\rangle = \begin{bmatrix} 0 \\ 0 \\ 0 \\ 1 \end{bmatrix}$$

7.6

Using the definitions in equation 7.1, sixteen product operators can be defined:

$$E(1)I(2) = E(1) \otimes I(2)$$

$$E(1)I_x(2) = E(1) \otimes I_x(2)$$

$$E(1)I_y(2) = E(1) \otimes I_y(2)$$

⋮

⋮

⋮

⋮

$$I_z(1)I_z(2) = I_z(1) \otimes I_z(2)$$

7.7

where the number in parenthesis indicates whether the operator acts on the first or the second spin function. Upon calculating the direct product of these operators, using the matrix representations given in equation 7.3 one obtains the matrix representations of the sixteen operators for a two spin system:

$$\begin{array}{cccc}
 & E_2 & I_{x2} & I_{y2} & I_{z2} \\
 E_1 & \begin{bmatrix} 1 & 0 & 0 & 0 \\ 0 & 1 & 0 & 0 \\ 0 & 0 & 1 & 0 \\ 0 & 0 & 0 & 1 \end{bmatrix} & \begin{bmatrix} 0 & 1 & 0 & 0 \\ 1 & 0 & 0 & 0 \\ 0 & 0 & 0 & 1 \\ 0 & 0 & 1 & 0 \end{bmatrix} & \begin{bmatrix} 0 & -i & 0 & 0 \\ i & 0 & 0 & 0 \\ 0 & 0 & 0 & -i \\ 0 & 0 & i & 0 \end{bmatrix} & \begin{bmatrix} 1 & 0 & 0 & 0 \\ 0 & -1 & 0 & 0 \\ 0 & 0 & 1 & 0 \\ 0 & 0 & 0 & -1 \end{bmatrix} \\
 I_{x1} & \begin{bmatrix} 0 & 0 & 1 & 0 \\ 0 & 0 & 0 & 1 \\ 1 & 0 & 0 & 0 \\ 0 & 1 & 0 & 0 \end{bmatrix} & \begin{bmatrix} 0 & 0 & 0 & 1 \\ 0 & 0 & 1 & 0 \\ 0 & 1 & 0 & 0 \\ 1 & 0 & 0 & 0 \end{bmatrix} & \begin{bmatrix} 0 & 0 & 0 & -i \\ 0 & 0 & i & 0 \\ 0 & -i & 0 & 0 \\ i & 0 & 0 & 0 \end{bmatrix} & \begin{bmatrix} 0 & 0 & 1 & 0 \\ 0 & 0 & 0 & -1 \\ 1 & 0 & 0 & 0 \\ 0 & -1 & 0 & 0 \end{bmatrix} \\
 I_{y1} & \begin{bmatrix} 0 & 0 & -i & 0 \\ 0 & 0 & 0 & -i \\ i & 0 & 0 & 0 \\ 0 & i & 0 & 0 \end{bmatrix} & \begin{bmatrix} 0 & 0 & 0 & -i \\ 0 & 0 & -i & 0 \\ 0 & i & 0 & 0 \\ i & 0 & 0 & 0 \end{bmatrix} & \begin{bmatrix} 0 & 0 & 0 & -1 \\ 0 & 0 & 1 & 0 \\ 0 & 1 & 0 & 0 \\ -1 & 0 & 0 & 0 \end{bmatrix} & \begin{bmatrix} 0 & 0 & -i & 0 \\ 0 & 0 & 0 & i \\ i & 0 & 0 & 0 \\ 0 & -i & 0 & 0 \end{bmatrix} \\
 I_{z1} & \begin{bmatrix} 1 & 0 & 0 & 0 \\ 0 & 1 & 0 & 0 \\ 0 & 0 & -1 & 0 \\ 0 & 0 & 0 & -1 \end{bmatrix} & \begin{bmatrix} 0 & 1 & 0 & 0 \\ 1 & 0 & 0 & 0 \\ 0 & 0 & 0 & -1 \\ 0 & 0 & -1 & 0 \end{bmatrix} & \begin{bmatrix} 0 & -i & 0 & 0 \\ i & 0 & 0 & 0 \\ 0 & 0 & 0 & i \\ 0 & 0 & -i & 0 \end{bmatrix} & \begin{bmatrix} 1 & 0 & 0 & 0 \\ 0 & -1 & 0 & 0 \\ 0 & 0 & -1 & 0 \\ 0 & 0 & 0 & 1 \end{bmatrix}
 \end{array}$$

7.8

When the elements of these matrices are arranged in row vectors and multiplied by the normalization factor  $\frac{1}{2}$ , the set of basis vectors  $U^{(j)}$  given in equation 1.18 are obtained.

APPENDIX II

## DERIVATION OF THE EXCHANGE OPERATOR,

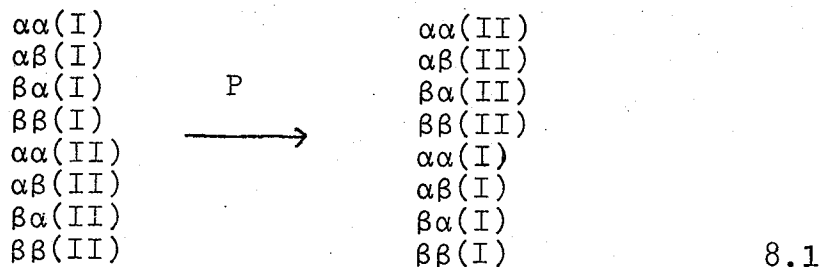
 $\chi$ , FOR A TWO SPIN SYSTEM.

The exchange operator,  $\chi$ , will not be derived for the most general case, but some justification for its form will be given by deriving it for an illustrative example, that of an AB spin system undergoing intramolecular exchange between two configurations. It will then be easy to see how it can be extended to more complicated systems.

The eight possible states of the spin system are:

$$\alpha\alpha(\text{I}), \alpha\beta(\text{I}), \beta\alpha(\text{I}), \beta\beta(\text{I}), \alpha\alpha(\text{II}), \alpha\beta(\text{II}), \beta\alpha(\text{II}), \beta\beta(\text{II}).$$

If it is assumed that the time taken for the exchange is small compared to the lifetime in a given configuration, then the spins remain correlated in time during the exchange, so that the effect of exchange will be:



Therefore we can write down the exchange operator P by inspection and represent the exchange as:

$$\begin{bmatrix}
 0 & 0 & 0 & 0 & 1 & 0 & 0 & 0 \\
 0 & 0 & 0 & 0 & 0 & 1 & 0 & 0 \\
 0 & 0 & 0 & 0 & 0 & 0 & 1 & 0 \\
 0 & 0 & 0 & 0 & 0 & 0 & 0 & 1 \\
 1 & 0 & 0 & 0 & 0 & 0 & 0 & 0 \\
 0 & 1 & 0 & 0 & 0 & 0 & 0 & 0 \\
 0 & 0 & 1 & 0 & 0 & 0 & 0 & 0 \\
 0 & 0 & 0 & 1 & 0 & 0 & 0 & 0
 \end{bmatrix}
 \begin{bmatrix}
 \alpha\alpha(I) \\
 \alpha\beta(I) \\
 \beta\alpha(I) \\
 \beta\beta(I) \\
 \alpha\alpha(II) \\
 \alpha\beta(II) \\
 \beta\alpha(II) \\
 \beta\beta(II)
 \end{bmatrix}
 =
 \begin{bmatrix}
 \alpha\alpha(II) \\
 \alpha\beta(II) \\
 \beta\alpha(II) \\
 \beta\beta(II) \\
 \alpha\alpha(I) \\
 \alpha\beta(I) \\
 \beta\alpha(I) \\
 \beta\beta(I)
 \end{bmatrix}$$

8.2

If the state of the system in configuration (I) is represented by the density matrix  $\rho^I$  and in configuration (II) by  $\rho^{II}$ , then the density matrix  $\rho$  for the total system, neglecting interaction between the two configurations, is:

$$\rho = \begin{bmatrix}
 \rho_{11}^I & \rho_{12}^I & \rho_{13}^I & \rho_{14}^I & 0 & 0 & 0 & 0 \\
 \rho_{21}^I & \rho_{22}^I & \rho_{23}^I & \rho_{24}^I & 0 & 0 & 0 & 0 \\
 \rho_{31}^I & \rho_{32}^I & \rho_{33}^I & \rho_{34}^I & 0 & 0 & 0 & 0 \\
 \rho_{41}^I & \rho_{42}^I & \rho_{43}^I & \rho_{44}^I & 0 & 0 & 0 & 0 \\
 0 & 0 & 0 & 0 & \rho_{11}^{II} & \rho_{12}^{II} & \rho_{13}^{II} & \rho_{14}^{II} \\
 0 & 0 & 0 & 0 & \rho_{21}^{II} & \rho_{22}^{II} & \rho_{23}^{II} & \rho_{24}^{II} \\
 0 & 0 & 0 & 0 & \rho_{31}^{II} & \rho_{32}^{II} & \rho_{33}^{II} & \rho_{34}^{II} \\
 0 & 0 & 0 & 0 & \rho_{41}^{II} & \rho_{42}^{II} & \rho_{43}^{II} & \rho_{44}^{II}
 \end{bmatrix}$$

8.3

$$P\rho P = \begin{bmatrix} \rho_{11}^{II} & \rho_{12}^{II} & \rho_{13}^{II} & \rho_{14}^{II} & 0 & 0 & 0 & 0 \\ \rho_{21}^{II} & \rho_{22}^{II} & \rho_{23}^{II} & \rho_{24}^{II} & 0 & 0 & 0 & 0 \\ \rho_{31}^{II} & \rho_{32}^{II} & \rho_{33}^{II} & \rho_{34}^{II} & 0 & 0 & 0 & 0 \\ \rho_{41}^{II} & \rho_{42}^{II} & \rho_{43}^{II} & \rho_{44}^{II} & 0 & 0 & 0 & 0 \\ 0 & 0 & 0 & 0 & \rho_{11}^I & \rho_{12}^I & \rho_{13}^I & \rho_{14}^I \\ 0 & 0 & 0 & 0 & \rho_{21}^I & \rho_{22}^I & \rho_{23}^I & \rho_{24}^I \\ 0 & 0 & 0 & 0 & \rho_{31}^I & \rho_{32}^I & \rho_{33}^I & \rho_{34}^I \\ 0 & 0 & 0 & 0 & \rho_{41}^I & \rho_{42}^I & \rho_{43}^I & \rho_{44}^I \end{bmatrix}$$

8.4

The effect of exchange on the time rate of change of the density matrix is given by:

$$\left(\frac{d\rho}{dt}\right)_{\text{exch.}} = (P\rho P - \rho)K, \quad 8.5$$

where  $K$  is the rate constant for the exchange. If the two configurations are unequally populated, then  $K_{12}$  will be different from  $K_{21}$ , and the effect on the equation of motion of the individual density matrices must be written separately. In that case

$$\left(\frac{d\rho^I}{dt}\right)_{\text{exchange}} = \Omega_1(P\rho P)K_{21} - \rho^I K_{12} \quad 8.6a$$

$$\left(\frac{d\rho^{II}}{dt}\right)_{\text{exchange}} = \Omega_2(P\rho P)K_{12} - \rho^{II} K_{21} \quad 8.6b$$

where  $\Omega_1$  and  $\Omega_2$  are projection operators, projecting the total density matrix into the subspaces of  $\rho^I$  and  $\rho^{II}$  respectively. We can see, for example, that the rate of change of  $\rho^I$  due to exchange depends on the rate  $K_{21}$  at which molecules from configuration II enter configuration I, and on  $K_{12}$  which is the rate at which molecules leave configuration I for configuration II. We can therefore write for the total system:

$$\left(\frac{d\rho}{dt}\right)_{\text{exchange}} = \begin{bmatrix} \begin{bmatrix} \rho^{II} K_{21} - \rho^I K_{12} & 0 & 0 & 0 \\ 0 & 0 & 0 & 0 \\ 0 & 0 & 0 & 0 \\ 0 & 0 & 0 & 0 \end{bmatrix} & \begin{bmatrix} 0 & 0 & 0 & 0 \\ 0 & 0 & 0 & 0 \\ 0 & 0 & 0 & 0 \\ 0 & 0 & 0 & 0 \end{bmatrix} \\ \begin{bmatrix} 0 & 0 & 0 & 0 \\ 0 & 0 & 0 & 0 \\ 0 & 0 & 0 & 0 \\ 0 & 0 & 0 & 0 \end{bmatrix} & \begin{bmatrix} \rho^I K_{12} - \rho^{II} K_{21} & 0 & 0 & 0 \\ 0 & 0 & 0 & 0 \\ 0 & 0 & 0 & 0 \\ 0 & 0 & 0 & 0 \end{bmatrix} \end{bmatrix} \quad 8.7$$

where  $\begin{bmatrix} \rho^{II} K_{21} - \rho^I K_{12} \\ 0 \\ 0 \\ 0 \end{bmatrix}$  and  $\begin{bmatrix} \rho^I K_{12} - \rho^{II} K_{21} \\ 0 \\ 0 \\ 0 \end{bmatrix}$  both represent 4 x 4 matrices.

In composite Liouville space, after arranging the matrix elements in the form of a column vector and omitting the zeros, one has:



$$\left( \frac{d\rho}{dt} \right)_{\text{exchange}} = \begin{bmatrix} \rho_{11}^{\text{II}} K_{21} - \rho_{11}^{\text{I}} K_{12} \\ \rho_{12}^{\text{II}} K_{21} - \rho_{12}^{\text{I}} K_{12} \\ \cdot \\ \cdot \\ \cdot \\ \cdot \\ \cdot \\ \cdot \\ \cdot \\ \rho_{44}^{\text{II}} K_{21} - \rho_{44}^{\text{I}} K_{12} \\ \rho_{11}^{\text{I}} K_{12} - \rho_{11}^{\text{II}} K_{21} \\ \rho_{12}^{\text{I}} K_{12} - \rho_{12}^{\text{II}} K_{21} \\ \cdot \\ \cdot \\ \cdot \\ \cdot \\ \cdot \\ \cdot \\ \rho_{44}^{\text{I}} K_{12} - \rho_{44}^{\text{II}} K_{21} \end{bmatrix}$$

8.8

In the Liouville representation, the effect of exchange on the equation of motion of  $\rho$  is written as:

$$\left( \frac{d\rho}{dt} \right)_{\text{exchange}} = \chi \rho$$

8.9

We can therefore write down the form of  $\chi$  by inspection:

	$11^I$	$12^I$		$44^I$	$11^{II}$	$12^{II}$		$44^{II}$		
$11^I$	$-K_{12}$	$0$	$\dots$		$K_{21}$	$0$	$\dots$		$\rho_{11}^I$	$\rho_{11}^{II} K_{21} - \rho_{11}^I K_{12}$
$12^I$	$0$	$-K_{12}$	$\dots$		$0$	$K_{21}$	$\dots$		$\rho_{12}^I$	$\rho_{12}^{II} K_{21} - \rho_{12}^I K_{12}$
	$\vdots$	$\vdots$	$\vdots$		$\vdots$	$\vdots$	$\vdots$		$\vdots$	$\vdots$
	$\vdots$	$\vdots$	$\vdots$		$\vdots$	$\vdots$	$\vdots$		$\vdots$	$\vdots$
$44^I$				$-K_{12}$	$0$	$\dots$	$\dots$		$\rho_{44}^I$	$\rho_{44}^{II} K_{21} - \rho_{44}^I K_{12}$
$11^{II}$	$K_{12}$	$0$	$\dots$		$0$	$-K_{21}$	$\dots$		$\rho_{11}^{II}$	$\rho_{11}^I K_{12} - \rho_{11}^{II} K_{21}$
$12^{II}$	$0$	$K_{12}$	$\dots$		$\vdots$	$-K_{21}$	$\dots$		$\rho_{12}^{II}$	$\rho_{12}^I K_{12} - \rho_{12}^{II} K_{21}$
	$\vdots$	$\vdots$	$\vdots$		$\vdots$	$\vdots$	$\vdots$		$\vdots$	$\vdots$
	$\vdots$	$\vdots$	$\vdots$		$\vdots$	$\vdots$	$\vdots$		$\vdots$	$\vdots$
$44^{II}$				$K_{12}$	$\dots$	$\dots$	$\dots$		$\rho_{44}^{II}$	$\rho_{44}^I K_{12} - \rho_{44}^{II} K_{21}$
				$\vdots$	$\vdots$	$\vdots$	$\vdots$		$\vdots$	$\vdots$

8.10

If there were several exchange processes taking place simultaneously, we would have to formulate the exchange operator  $P$  separately for each exchange, and equations (8.6) would be generalized to:

$$\begin{aligned} \left( \frac{d\rho^I}{dt} \right)_{\text{exchange}} &= \Omega_1 [(P^{12} \rho P^{12})_{K_{21}} + (P^{13} \rho P^{13})_{K_{31}} + \dots + (P^{1n} \rho P^{1n})_{K_{n1}}] \\ &\quad - \rho^I (K_{12} + K_{13} + \dots + K_{1n}) \\ \left( \frac{d\rho^{II}}{dt} \right)_{\text{exchange}} &= \Omega_2 [(P^{12} \rho P^{12})_{K_{12}} + \dots + (P^{n2} \rho P^{n2})_{K_{n2}}] \\ &\quad - \rho^{II} (K_{21} + K_{23} + \dots + K_{2n}) \\ &\quad \cdot \\ &\quad \cdot \\ &\quad \cdot \\ &\quad \cdot \\ \left( \frac{d\rho^n}{dt} \right)_{\text{exchange}} &= \Omega_n [(P^{1n} \rho P^{1n})_{K_{1n}} + (P^{2n} \rho P^{2n})_{K_{2n}} + \dots + (P^{(n-1)n} \rho P^{(n-1)n})_{K_{(n-1)n}}] \\ &\quad - \rho^n (K_{n1} + K_{n2} + \dots + K_{n(n-1)}) \end{aligned} \quad 8.11$$

The exchange operator  $\chi$  can be set up in a fashion similar to that used for the two-configuration case, and it will consist of  $n^2$  blocks for an  $n$  configuration system, with each block having as diagonal elements the appropriate rate constants. Thus the general form of  $\chi$  will be:

$$\chi_{\mu_r \nu_r, \lambda_s \kappa_s} = \delta_{\mu\kappa} \delta_{\nu\lambda} \left[ -\delta_{rs} \sum_{t \neq r} K_{rt} + (1 - \delta_{rs}) K_{sr} \right], \quad 8.12$$

where the subscripts  $r$  and  $s$  are labels for the configurations.